Toward an Understanding of the High Enantioselectivity in the Osmium-Catalyzed Asymmetric Dihydroxylation. 4. Electronic Effects in Amine-Accelerated Osmylations

Derek W. Nelson,[†] Andreas Gypser,[†] Pui Tong Ho,[†] Hartmuth C. Kolb,[†] Teruyuki Kondo,[†] Hoi-Lun Kwong,[†] Dominic V. McGrath,[†] A. Erik Rubin,[†] Per-Ola Norrby,[§] Kevin P. Gable,[‡] and K. Barry Sharpless*,[†]

Contribution from the Department of Chemistry, The Scripps Research Institute, 10550 North Torrey Pines Road, La Jolla, California 92037, Royal Danish School of Pharmacy, Department of Chemistry, Universitetsparken 2, DK-2100 Copenhagen, Denmark, and Department of Chemistry, Oregon State University, Corvallis, Oregon 97331-4003

Received May 2, 1996[⊗]

Abstract: Electronic effects in osmylation reactions accelerated by pyridine and quinuclidine derivatives were investigated by varying the substituents on the amine ligand as well as on the alkene substrate. Ligand substituent effects were gauged by determination of the equilibrium constants for coordination of the amines to OsO_4, evaluation of structural properties and reduction potentials of the amine−OsO_4 complexes, and analysis of the kinetics of osmylations in the presence of the amines. Substrate substituent effects were gauged by kinetic Hammett studies using several different amine/alkene combinations. Nonlinear Hammett relationships resulting from alkene substituent effects were observed, and the deviation from a linear free energy relationship was found to depend on the structure, binding capacity, and concentration of the amine. The results were evaluated in terms of the contending "[3 + 2]" and "[2 + 2]" mechanisms currently under consideration. A change in mechanism that depends on the structural and electronic properties of both alkene and amine is proposed.

Introduction

The osmium-catalyzed asymmetric dihydroxylation (AD) has become one of the most general and efficient methods available to the synthetic organic chemist.[1] In spite of the widespread use of the AD, certain aspects of the reaction, notably the specifics of the process by which two of the oxo groups of osmium tetroxide form bonds to the carbon atoms of the alkene and the nature of the noncovalent interactions responsible for the high levels of asymmetric induction, remain the subject of debate. Chiral alkaloid derivatives that coordinate to osmium tetroxide through the nitrogen of a quinuclidine moiety provide the ligand acceleration and asymmetric induction in the AD,[2] but the complex conformational changes and noncovalent interactions that occur in the transition state assembly make it very difficult to analyze any one specific aspect of the reaction mechanism. As part of continuing efforts to better understand this complex reaction, the kinetic role of sterically undemanding tertiary amines and various other ligands capable of accelerating osmylations has been reinvestigated.[3] Until the mechanistic details of the simplest ligand-accelerated osmylations are known, studies on the asymmetric versions of the reaction, no matter how sophisticated, must be considered speculative.

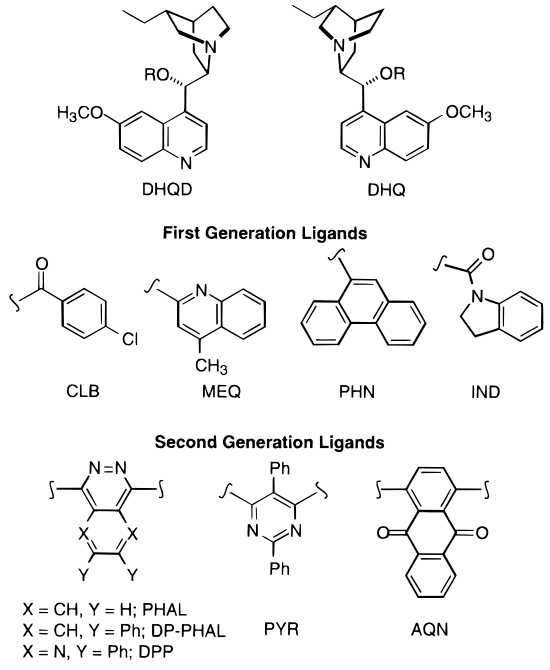

Monodentate tertiary amines, regardless of basicity or steric environment, coordinate to OsO_4 in organic solvents to form a 1:1 complex, and the rate of osmylation reaches saturation at high amine concentrations. Extensive kinetic analyses of both catalytic and stoichiometric dihydroxylations show that only a single amine is involved in the transition state of the rate-determining step.[2,4] An exception to this behavior occurs in buffered aqueous systems where the kinetics are described by

[†] The Scripps Research Institute.
[‡] Royal Danish School of Pharmacy.
[§] Oregon State University.
[⊗] Abstract published in *Advance ACS Abstracts,* January 15, 1997.

(1) Kolb, H. C.; VanNieuwenzhe, M. S.; Sharpless, K. B. *Chem. Rev.* **1994**, *94*, 2483.

(2) (a) Jacobsen, E. N.; Markó, I.; Mungall, W. S.; Schröder, G.; Sharpless, K. B. *J. Am. Chem. Soc.* **1988**, *110*, 1968. (b) Jacobsen, E. N.; Markó, I.; France, M.; Svendsen, J. S.; Sharpless, K. B. *J. Am. Chem. Soc.* **1989**, *111*, 737. (c) Kolb, H. C.; Andersson, P. G.; Sharpless, K. B. *J. Am. Chem. Soc.* **1994**, *116*, 1278.

(3) A wide variety of ligands including acetate, halides, and azide have been found to accelerate stoichiometric osmylation reactions: Sharpless, K. B.; Walsh, P. J. Unpublished results.

(4) Kolb, H. C.; Andersson, P. G.; Bennani, Y. L.; Crispino, G. A.; Jeong, K.-Y.; Kwong, H.-L.; Sharpless, K. B. *J. Am. Chem. Soc.* **1993**, *115*, 12226.

S0002-7863(96)01464-3 CCC: $14.00

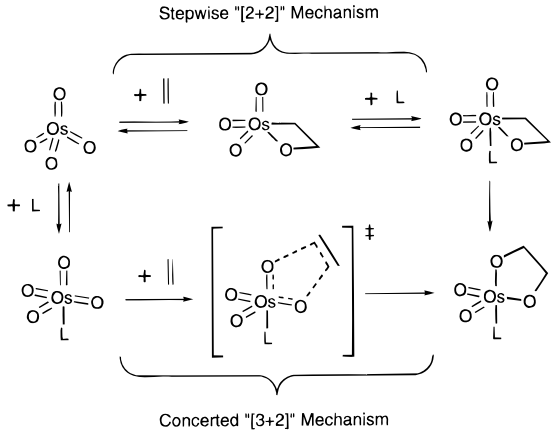

Figure 1. Proposed mechanisms for the amine-accelerated osmylation of alkenes (L = tertiary amine).

a different rate expression that exhibits a second-order dependence on amine concentration.[5,6] Several different OsO_4 complexes involving two coordinating amines have been proposed as reactive intermediates.[6,7] Vicinal diamine ligands that can afford stoichiometric asymmetric osmylation of alkenes have been developed,[8] but the kinetics of these reactions have not been studied.

Two distinct reaction pathways have been proposed to account for the formation of osmium(VI) glycolates in the presence of monodentate coordinating tertiary amines: a concerted reaction mechanism involving a pericyclic transition state (the "[3 + 2]" pathway)[9] and a stepwise route involving formation of an osmaoxetane from *formal* [2 + 2] addition of the alkene to OsO_4 (Figure 1).[10,11] Both of the proposed pathways can explain the most important features of the reaction, including the net suprafacial addition of the two oxygens to the alkene, the distinctive kinetic behavior, and the pattern of facial selectivity observed using chiral alkaloid ligands. To date, mechanistic studies have not provided definitive evidence for either of the proposed pathways. However, the discovery of inversion points in modified Eyring plots of enantioselectivity as a function of temperature is inconsistent with a simple concerted process.[12] Computational studies have indicated that formation of ligated metallaoxetanes is endothermic, but the structures represent minima on energy hypersurfaces and are consistent with the experimentally observed pattern of facial selectivity.[13] Unequivocal evidence for the existence of a reactive intermediate remains elusive, however.

Numerous attempts to probe the mechanism of osmylation through the pairing of sterically encumbered alkenes and/or amine ligands have been made. A related approach employing substituents at sites remote from the reactive centers yet capable of directly influencing the energies of the reactive orbitals on both the alkene and amine should provide important information about the nature of the reactive species. The extensive use of electronic perturbation as a probe to elucidate mechanistic details has resulted in the development of empirical parameters, usually variants of the σ and ρ parameters developed by Hammett, that can be used to assess the influence of different substituents on kinetic and thermodynamic phenomena.[14] A thorough investigation of electronic effects in osmylation reactions has not yet appeared, but a few studies on substituent effects in osmylations have been reported. A slight substituent effect on the rate of pyridine-accelerated dihydroxylation of aromatic compounds by OsO_4 was observed in early work.[15] Subsequently, Henbest reported a linear correlation between the Hammett σ values of symmetrically substituted *trans*-stilbenes and the rates of osmylation *in the absence of amine ligands*.[16] Electron-donating substituents on the stilbenes resulted in faster reaction rates, and a ρ value of -0.55 was determined. A similar study on the relative rates of reaction of *tert*-butylimidotrioxoosmium(VIII) with substituted α-methylstyrenes revealed a *nonlinear* relationship between the σ values of the aromatic substituents and the reaction rate; both electron-donating and -withdrawing substituents on the phenyl group of the alkene accelerated reaction rates.[17] The reactivity of imidotrioxoosmium(VIII) complexes with alkenes has been proposed to be closely related to that of OsO_4. Mixtures of the vicinal diol and the vicinal hydroxyamine derivatives are produced in the former, and coordinating tertiary amines can dramatically alter the product distribution.[18]

Several reports of electronic and stereoelectronic effects on turnover or product distribution in osmium-catalyzed dihydroxylations using tertiary amine *N*-oxides as stoichiometric oxidants have appeared in the literature.[19] The structure of the substrate plays an important role in the selectivity of catalytic osmylation reactions,[1] particularly in the diastereoselectivity of the reaction. Empirical models that predict the influence of allylic substituents on facial selectivity in osmium-catalyzed dihydroxylations have been proposed.[20] Mechanistic interpreta-

(5) Burton, K. *Biochem. J.* **1967**, *104*, 686.

(6) Subbaraman, L. R.; Subbaraman, J.; Behrman, E. J. *Bioinorg. Chem.* **1971**, *1*, 35. (b) Subbaraman, L. R.; Subbaraman, J.; Behrman, E. J. *Inorg. Chem.* **1972**, *11*, 2621. (c) Clark, R. L.; Behrman, E. J. *Inorg. Chem.* **1975**, *14*, 1425.

(7) Jørgensen, K. A.; Hoffmann, R. *J. Am. Chem. Soc.* **1986**, *108*, 1867.

(8) (a) Yamada, T.; Narasaka, K. *Chem. Lett.* **1986**, 131. (b) Tokles, M.; Snyder, J. K. *Tetrahedron. Lett.* **1986**, *27*, 3951. (c) Tomioka, K.; Nakajima, M.; Koga, K. *J. Am. Chem. Soc.* **1987**, *109*, 6213. (d) Tomioka, K.; Nakajima, M.; Iitaka, Y.; Koga, K. *Tetrahedron Lett.* **1988**, *29*, 573. (e) Tomioka, K.; Nakajima, M.; Koga, K. *Tetrahedron Lett.* **1990**, *31*, 1741. (f) Nakajima, M.; Tomioka, K.; Iitaka, Y.; Koga, K. *Tetrahedron* **1993**, *49*, 10793. (g) Corey, E. J.; Jardine, P. D.; Virgil, S.; Yuen, P.-W.; Connell, R. D. *J. Am. Chem. Soc.* **1989**, *111*, 9243. (h) Hirama, M.; Oishi, T.; Oishi, T.; Itô, S. *J. Chem. Soc., Chem. Commun.* **1989**, 665. (i) Oishi, T.; Hirama, M. *J. Org. Chem.* **1989**, *54*, 5834. (j) Fuji, K.; Tanaka, K.; Miyamoto, H, *Tetrahedron Lett.* **1992**, *33*, 4021. (k) Hannessian, S.; Meffre, P.; Girard, M.; Beaudoin, S.; Sancéau, J.-Y.; Bennani, Y. L. *J. Org. Chem.* **1993**, *58*, 1991.

(9) (a) Böseken, J. *Recl. Trav. Chim.* **1922**, *41*, 199. (b) Criegee, R. *Justus Liebigs Ann. Chem.* **1936**, *522*, 75. (c) Dewar, M. J. S. *J. Am. Chem. Soc.* **1952**, *74*, 3357. (d) Corey, E. J.; Noe, M. C. *J. Am. Chem. Soc.* **1993**, *115*, 1279. A variation of the classical "[3 + 2]" pathway involving a rapid and reversible equilibrium between the alkene and $L-OsO_4$ has recently been postulated by Corey (*vide infra*).

(10) (a) Sharpless, K. B.; Teranishi, A. Y.; Bäckvall, J.-E. *J. Am. Chem. Soc.* **1977**, *99*, 3120. (b) For recent developments in this model, see: Norrby, P.-O.; Becker, H.; Sharpless, K. B. *J. Am. Chem. Soc.* **1996**, *118*, 35.

(11) For a general review of metalloxetanes, see: Jørgensen, K. A.; Schiøtt, B. *Chem. Rev.* **1990**, *90*, 1483.

(12) (a) Göbel, T.; Sharpless, K. B. *Angew. Chem., Int. Ed. Engl.* **1993**, *32*, 1329. (b) Additional studies indicate that inversion points exist in modified Eyring plots based on chemoselectivity for unaccelerated and pyridine-accelerated osmylations: McGrath, D. V.; Makita, A.; Sharpless, K. B. Unpublished results.

(13) (a) Veldkamp, A.; Frenking, G. *J. Am. Chem. Soc.* **1994**, *116*, 4937. (b) Norrby, P.-O.; Kolb, H. C.; Sharpless, K. B. *Organometallics* **1994**, *13*, 344. (c) Norrby, P.-O.; Kolb, H. C.; Sharpless, K. B. *J. Am. Chem. Soc.* **1994**, *116*, 8470.

(14) Hansch, C.; Leo, A.; Taft, R. W. *Chem. Rev.* **1991**, *91*, 165 and references cited therein.

(15) (a) Badger, G. M. *J. Chem. Soc.* **1949**, 456. (b) Badger, G. M.; Lynn, K. R. *J. Chem. Soc.* **1950**, 1726.

(16) Henbest, H. B.; Jackson, W. R.; Robb, B. C. G. *J. Chem. Soc B* **1966**, 804.

(17) Patrick, D. W.; Truesdale, L. K.; Biller, S. A.; Sharpless, K. B. *J. Org. Chem.* **1978**, *43*, 2628.

(18) Hentges, S. G.; Sharpless, K. B. *J. Org. Chem.* **1980**, *45*, 2257.

(19) For representative examples, see: (a) Vedejs, E.; Dent, W. H. *J. Am. Chem. Soc.* **1989**, *111*, 6861. (b) Burdisso, M.; Gandolfi, R.; Rastelli, A. *Tetrahedron Lett.* **1991**, 2659. (c) Vedejs, E.; Dent, W. H., III; Kendall, J. T.; Oliver, P. A. *J. Am. Chem. Soc.* **1996**, *118*, 3556.

(20) (a) Hoveyda, A. H.; Evans, D. A.; Fu, G. C. *Chem. Rev.* **1993**, *93*, 1307. (b) Cha, J. K.; Kim, N.-S. *Chem. Rev.* **1995**, *95*, 1761.

tions based on product distributions in catalytic dihydroxylations using tertiary amine *N*-oxide cooxidants are speculative, at best, because the catalytic cycle comprises several poorly defined steps. Evidence for the participation of two different Os(VIII) oxidants in *N*-methylmorpholine *N*-oxide (NMO) based catalytic osmylations has been presented, but little is known about the intermediates in the proposed "second cycle".[21]

The work presented here describes the first thorough study of electronic effects in stoichiometric amine-accelerated osmylation reactions. The influence of substituents that alter the electronic properties of both the alkene and the accelerating tertiary amine has been systematically determined. Amines such as 4-substituted pyridines do not create a complex steric environment near the site of coordination and provide an excellent opportunity to probe the mechanism by analysis of subtle electronic effects. Amine substituent effects were probed by measurement of the binding constants for the equilibrium between the tertiary amines and OsO_4 as well as by investigation of the kinetic behavior of the ligands. Electrochemical data and X-ray crystal structures of certain amine−OsO_4 complexes were determined to complete the investigation of ligand effects. Substrate electronic effects were evaluated using readily available aryl-substituted olefins, and the kinetics of a wide variety of amine-alkene combinations were studied. A brief investigation of the influence of substrate electronic effects on enantioselectivity in stoichiometric and catalytic versions of the AD is also reported.

Determination of Equilibrium Constants for Amine−Osmium Tetroxide Complexes and Measurement of Osmylation Rates. The coordination of tertiary amines to OsO_4 is well established. The 18-electron complex between pyridine and OsO_4 was prepared by Criegee,[22] and the quinuclidine−OsO_4 complex was prepared and characterized by Griffith in 1977.[23] The OsO_4 complex with the modified alkaloid ligand DHQD-CLB was reported soon after the discovery of the NMO-based version of the AD.[24] Equilibrium constants for the binding of osmium tetroxide to quinuclidine derivatives and alkaloid ligands in different solvents have been reported.[2c] Surprisingly, no simple correlation exists between the binding constant and the rate of osmylation at ligand saturation for ligands that coordinate to osmium through the nitrogen of a quinuclidine moiety. For example, quinuclidine coordinates very strongly to OsO_4 (K_{eq} ~80 000 M^{-1} in toluene at 25 °C) but accelerates the rate of osmylation much less than DHQD-CLB (K_{eq} = 56 M^{-1} in toluene at 25 °C).[2c] The bisalkaloid AD ligands such as $(DHQD)_2PHAL$ bind even more poorly to osmium tetroxide and yet cause remarkable rate enhancements, often in the range of 10^3-10^4 compared to the background reaction, in the osmylation of alkenes with aromatic substituents. A "binding pocket" resulting from favorable noncovalent interactions between the aromatic π systems of the substrate and the alkaloid ligand has been proposed to account for both rate acceleration and facial selectivity,[2c,25] but controversy over the orientation of alkenes such as styrene in the transition state has arisen.[26]

Scheme 1

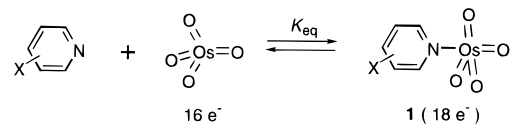

Table 1. Equilibrium Constants for the Binding of Substituted Pyridines to OsO_4 in Organic Solvents (Scheme 1)

pyridine substituent (X)	σ^a	K_{eq} (M^{-1}) acetonitrile	K_{eq} (M^{-1}) toluene
4-$N(CH_3)_2$	−0.83	1200 ± 90	1820 ± 230
3,4-$(CH_2)_4$	−0.48	143 ± 2	402 ± 100
4-CH_3	−0.17	70 ± 3	163 ± 30
none	0.00	34 ± 2	79 ± 7
3-F	0.34	4.1 ± 0.6	17 ± 1
4-CN	0.66	2.0 ± 1.0	4.4 ± 0.8
3,5-$(Cl)_2$	0.74[b]		2.0 ± 1.4

[a] The σ_m parameter was used for substituents at C(3), and the σ_p parameter was used for substituents at C(4). [b] This substituent parameter was obtained by adding the individual σ_m values for both substituents.[27]

In order to simplify the analysis of substituent effects, initial studies were performed using substituted pyridines as ligands in stoichiometric osmylation reactions. The coordination of sterically simple amines is not complicated by factors such as the change from the "closed" to the "open" conformation[24] that necessarily occurs upon complexation of derivatized alkaloids to OsO_4, so it is easier to gauge the electronic effects in both the OsO_4−ligand equilibrium and the osmylation transition state. The equilibrium constants for the coordination of the substituted pyridines to OsO_4 were measured by a spectrophotometric method. Free osmium tetroxide and its complex with a tertiary amine exhibit different absorbances in the UV−visible spectrum, and the equilibrium constants for the complexation were determined by monitoring the spectral changes as a dilute solution of OsO_4 was titrated with a solution of the amine. The binding constants, calculated by both single- and double-reciprocal graphical methods developed for a 1:1 binding isotherm,[28] for the series of pyridine derivatives in acetonitrile and toluene are listed in Table 1. Hammett plots for the two series of equilibria exhibit linear relationships using the standard σ values[29] for the substituent parameters, and ρ values of −1.8 and −1.9 were obtained for the equilibria in acetonitrile and toluene, respectively. The ρ values differ insignificantly in spite of the marked difference in polarity between acetonitrile (ϵ = 36.2,[30] $E_T(30)$ = 45.6 kcal/mol[31]) and toluene (ϵ = 2.38,[30] $E_T(30)$ = 33.9 kcal/mol[31]).

The ρ values for the plots shown in Figure 2 have absolute magnitudes >1 indicating that the equilibrium is more sensitive

(21) Wai, J. S. M.; Markó, I.; Svendsen, J. S.; Finn, M. G.; Jacobsen, E. N.; Sharpless, K. B. *J. Am. Chem. Soc.* **1989**, *111*, 1123.

(22) Criegee, R.; Marchand, B.; Wannowius, H. *Justus Liebigs Ann. Chem*. **1949**, *550*, 99.

(23) (a) Griffith, W. P.; Skapski, A. C.; Woode, K. A.; Wright, M. J. *Inorg. Chim. Acta* **1978**, *31*, L413. (b) Cleare, M. J.; Hydes, P. C.; Griffith, W. P.; Wright, M. J. *J. Chem. Soc., Dalton Trans.* **1977**, 941.

(24) Svendsen, J. S.; Markó, I.; Jacobsen, E. N.; Rao, C. P.; Bott, S.; Sharpless, K. B. *J. Org. Chem.* **1989**, *54*, 2263.

(25) (a) Becker, H.; Ho, P. T.; Kolb, H. C.; Loren, S.; Norrby, P.-O.; Sharpless, K. B. *Tetrahedron Lett.* **1994**, *35*, 7315. (b) Becker, H.; Soler, M. A.; Sharpless, K. B. *Tetrahedron* **1995**, *51*, 1345.

(26) For examples of models based on the "[3 + 2]" pathway, see: (a) Corey, E. J.; Noe, M. C. *J. Am. Chem. Soc.* **1993**, *115*, 12579. (b) Corey, E. J.; Noe, M. C.; Sarshar, S. *Tetrahedron Lett.* **1994**, *35*, 2861. (c) Corey, E. J.; Noe, M. C.; Grogan, M. J. *Tetrahedron Lett.* **1994**, *35*, 6427. (d) Corey, E. J.; Guzman-Perez, A.; Noe, M. C. *J. Am. Chem. Soc.* **1994**, *116*, 12109. (e) Corey, E. J.; Guzman-Perez, A.; Noe, M. C. *J. Am. Chem. Soc.* **1995**, *117*, 10805. (f) Corey, E. J.; Noe, M. C.; Guzman-Perez. A. *J. Am. Chem. Soc.* **1995**, *117*, 10817.

(27) For a discussion of the additivity of substituent parameters, see: Stone, R. M.; Pearson, D. E. *J. Org. Chem.* **1961**, *26*, 257.

(28) Conners, K. A. *Binding Constants*; John Wiley & Sons: New York, 1987; pp 141−160.

(29) An alternate series of Hammett σ parameters derived by NMR methods exists, but these values afford a poorer correlation for a linear fit to the data in Figure 2. For a discussion of alternate parameters, see: March, J. *Advanced Organic Chemistry: Reactions, Mechanism, and Structure*, 4th ed.; John Wiley & Sons: New York, 1992; pp 278−286.

(30) Gordon, A. J.; Ford, R. A. *The Chemist's Companion*; John Wiley & Sons: New York, 1972; p 123.

(31) Reichardt, C. *Chem Rev.* **1994**, *94*, 2319.

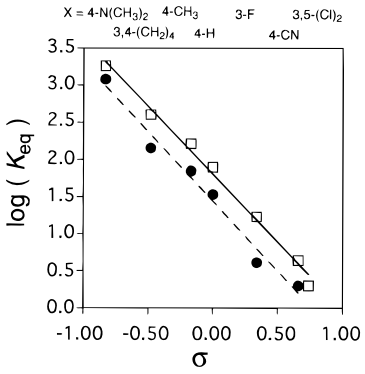

Figure 2. Hammett plots based on the equilibrium constants for the binding of substituted pyridines to OsO_4 in acetonitrile (-●-: $\rho = -1.8$, $r = 0.996$) and toluene (-□-: $\rho = -1.9$, $r = 0.991$) at 25.0 °C.

Scheme 2

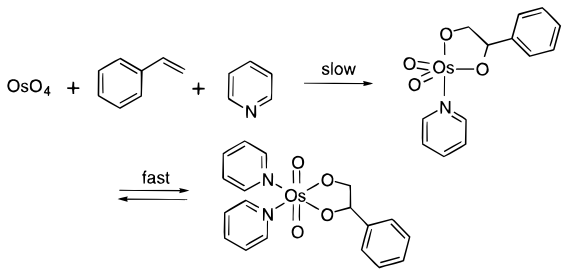

to electronic effects than the ionization of benzoic acids. For comparison, a Hammett plot of the pK_a's of the protonated pyridines in water vs the σ parameters for the substituents is linear and yields a ρ value of -6.[32] A substantial amount of charge separation upon formation of complex **1** is implied from the data in Table 1, and the electrophilicity of the metal center in OsO_4 is clearly demonstrated. The two organic solvents employed for the binding constant determinations were used for the majority of the kinetic work discussed here so that complications, such as acid−base equilibria and hydrogen-bonding in the protic solvents employed in the catalytic AD, could be avoided. In addition, kinetic analysis was straightforward in both solvents.

The kinetic behavior of substituted pyridines as ligands for osmylation in organic solvents is identical to that of the alkaloid ligands; a single amine participates in the rate-determining step, both types of amines accelerate the rate of formation of osmium(VI) glycolates, and rate saturation at high amine concentrations occurs.[3,8] The key step in the pathway, formation of the monopyridine osmium(VI) glycolate, can be monitored by following the rate of formation of the dipyridine osmium(VI) glycolates because the coordination of the second amine is rapid and reversible (Scheme 2). Figure 3 shows a typical rate profile for pyridine-accelerated osmylations as the concentration of the amine is increased. A comparison of the capacity of differently substituted pyridines to accelerate the osmylation of a particular alkene must utilize the "ceiling" rate constants (k_c) corresponding to the reaction rates at ligand saturation, particularly if the equilibrium constants for the amines are very different. The k_c values are calculated using eq 1 that requires the experimentally determined equilibrium constant (K_{eq}) and several experimentally determined rate constants (k_{obs}) corresponding to points on the saturation curve.[33] The rate constant k_1 describes the rate-determining step for the concerted addition of the amine−

(32) The following pK_a values for protonated substituted pyridines were used in this Hammett analysis: 4-N$(CH_3)_2$, 10.5; 4-NH_2, 9.2; 4-CH_3, 6.0; 4-Cl, 3.8; 3-Cl, 2.8.

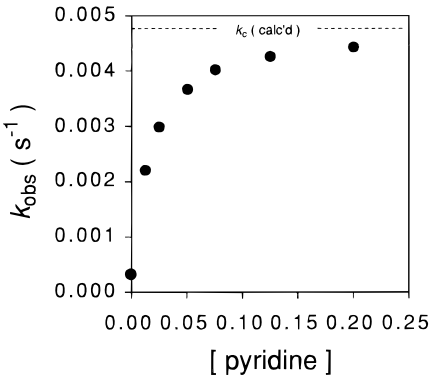

Figure 3. Saturation rate curve for the pyridine-accelerated reaction of OsO_4 (2.0×10^{-4} M) with styrene (4.0×10^{-3} M) in toluene at 25 °C.

Table 2. Calculated Ceiling Rate Constants for the Substituted-Pyridine Accelerated Osmylation of Styrene in Toluene at 25.0 °C

pyridine substituent	k_c (M^{-1} s^{-1})[a]
4-N$(CH_3)_2$	1.7
4-CH_3	1.4
none	1.2
3-F	0.7
4-CN	1.1
3,5-$(Cl)_2$	0.6

[a] The concentrations of the pyridines used ranged from 1.25−25.0 $\times 10^{-2}$ M ($[OsO_4]_o = 2.0 \times 10^{-4}$ M, $[styrene]_o = 4.0 \times 10^{-3}$ M). The k_c values were obtained from plots of $k_{obs}(1 + K_{eq}[L])$ vs [L] and have estimated errors of ±10% for the strongly binding amines and ±25 for poorly binding amines.

OsO_4 complex to the alkene in Figure 1. The concentration of osmium tetroxide ($[OsO_4]_T$) represents the sum of the concentrations of the free and amine-complexed forms. A kinetically

$$\text{rate} = k_{obs}[OsO_4]_T[\text{alkene}] \quad \text{AND}$$

$$k_c = \underbrace{\left[\frac{k_o + k_1 K_{eq}[L]}{1 + K_{eq}[L]}\right]}_{k_{obs}} \lim_{[L]\to\infty} \qquad (1)$$

indistinguishable form of the rate expression can be derived for the stepwise "[2 + 2]" pathway (vide supra), and previous work has shown that the form of the rate expression cannot be used to distinguish between the two mechanistic possibilities.[2] The rate of osmylation in the absence of amine (k_o) is not necessary for the graphical technique used to obtain the ceiling rate constant, but it is necessary for the determination of the extent of ligand acceleration at rate saturation.

The influence of the pyridine substituent effects on ceiling rate constants was determined by undertaking a Hammett study employing several of the pyridine derivatives listed in Table 1 to accelerate the osmylation of styrene in toluene. The extrapolated ceiling rate constants are listed in Table 2. With the exception of the reactions accelerated by 4-cyanopyridine, a monotonic decrease is observed in the saturation rate constants as the equilibrium constant for the

(33) Derivations of the rate expressions corresponding to the different mechanisms are included in the Supporting Information.

Table 3. Equilibrium Constants for the Binding of Substituted Quinuclidines to OsO_4 in Toluene and Corresponding Ceiling Rate Constants for the Osmylation of Cyclohexene in Toluene at 25.0 °C[a]

C(4) substituent	$\sigma_{I(q)}$	$10^4 \times K_{eq}$ (M^{-1})[b]	k_c (M^{-1} s^{-1})[b]
H	0.0	8.0	38.6
CH_3	0.11	6.9	48.1
CH_2OCH_3	0.66	6.0	49.1
C_6H_5	0.94	5.3	52.8
OSO_2-*p*-$(CH_3)C_6H_4$	1.28	2.9	54.9
$CO_2CH_2CH_3$	1.70	2.3	53.3
OCH_3	1.81	2.5	53.9
O_2CCH_3	2.12	1.3	55.4

[a] $[OsO_4]_o = 2.0 \times 10^{-3}$ M, $[\text{cyclohexene}]_o \geq 8.0 \times 10^{-2}$ M. [b] Errors in the K_{eq} and k_c values are estimated to be ±10%.

binding of the amines to OsO_4 decreases. An attempt to determine a correlation with the Hammett substituent parameter resulted in a poor linear fit of the data ($r = 0.82$), and the ρ value of −0.2 calculated from a Hammett analysis of the data in Table 2 has a large associated error. Strongly coordinating pyridines afford faster reaction rates under these experimental conditions, but this study shows that relatively small differences exist between the ceiling rate constants calculated for strongly and weakly binding amines. The extrapolated k_c value for the 4-cyanopyridine-accelerated series is higher than expected based on the equilibrium constants for formation of the amine−OsO_4 complex. The explanation for this anomaly remains unclear. The experimentally determined rates used to calculate the ceiling rate constant are close to the saturation values for the pyridines with electron-donating substituents. The experimental rates used to calculate the ceiling rate constants for the poorly binding amines are only at ∼50% of the saturation rates, however. Any deviation from linearity in a Hammett plot based on the data in Table 2, particularly that corresponding to the data for the poorly binding pyridines, may be attributed to the error introduced by extrapolation.

The influence of the amine's substituents on the ceiling rate constants of osmylation was further investigated by studying the ligand-acceleration in osmylation using 4-substituted quinuclidines. Grob developed a series of parameters ($\sigma_{I(q)}$) specifically for the inductive effects caused by substituents at the carbon bridgehead in quinuclidine derivatives.[34] A series of these quinuclidines was prepared by simple modification of Grob's procedures,[35] and the kinetic function of these amines in osmylation reactions was studied. Initially, the equilibrium constants for the coordination of the quinuclidines were measured. The extremely large binding affinities of the quinuclidines prevented use of the UV−visible method employed with the pyridine derivatives, so the equilibrium constants were measured by competition experiments using an NMR technique. All of the substituted quinuclidines coordinated less strongly to OsO_4 than quinuclidine itself, and the equilibrium constants obeyed an approximately linear Hammett relationship with a ρ value of −0.3 ($r = 0.96$). The experimental rate constants obtained using modest excesses of the quinuclidines are essentially the ceiling rates, so the error introduced by extrapolation is minimal. A Hammett plot based on the k_c values for the substituted-quinuclidine accelerated osmylations of cyclohexene was linear ($r = 0.97$), and the ρ value of 0.04 is again very small. It is important to note that the ceiling rates for the substituted-quinuclidine reactions listed in Table 3 *increase* as the equilibrium constant for coordination to OsO_4 decreases.

(34) Grob, C. A.; Schlageter, M. G. *Helv. Chim. Acta* **1976**, *59*, 264.
(35) Eckhardt, W.; Grob, C. A.; Treffert, W. D. *Helv. Chim. Acta* **1972**, *35*, 2432.

Substituents at remote positions of the coordinating amines play an important role in the capacity of the amine to coordinate to OsO_4. Within a series of related tertiary amines where the environment near the coordinating nitrogen atom does not change, the equilibrium constants for binding to OsO_4 increase as the basicity of the amine increases. The influence of the amine's substituent on the ceiling rate constants for osmylation of alkenes is not as straightforward. As illustrated in Tables 1 and 2, the saturation rates of the styrene reactions accelerated by substituted pyridines differ by a factor of three, whereas the binding constants differ by three orders of magnitude. The equilibrium constants for coordination of the 4-substituted quinuclidines differ by less than on order of magnitude. The effect of the quinuclidine substituents on the ceiling rates of osmylations is not only very small (Table 3), but opposite that observed with the pyridines. Thus, the electronic nature of the amine substituent dramatically influences the binding constants for both pyridines and quinuclidines, but the effect on the rate of osmylation at ligand saturation is surprisingly small and not consistent for structurally different amines.

Electrochemical and Structural Studies of Amine−OsO_4 Complexes. The data describing the influence of amine substituents on the equilibrium constants and the ceiling rates of osmylations can be used to evaluate the proposed mechanisms. If the "[3 + 2]" mechanism operates, then the saturation rates should correspond to the rate of reaction of the amine−OsO_4 complex **1** with the alkene thereby eliminating any component arising from the different K_{eq} values. Examination of amine substituent effects on the structure and energetics of complex **1** is required to determine whether the small rate differences shown in Tables 2 and 3 are consistent with a reaction via this species. The pyridine substituent not only should influence the equilibrium for the coordination to OsO_4 but also should influence the energy levels of the orbitals on the OsO_4−ligand complex. Specifically, any coordinated tertiary amine should decrease the Lewis acidity of osmium tetroxide, and the resulting 18-electron complex should be more difficult to reduce than free OsO_4. The monoamine complex should therefore be a *less* efficient oxidizing agent as a result of this change in reduction potential. Similarly, amine substituents exert a direct influence on the capacity of the amines to coordinate to OsO_4 and should also influence the orbital energies of complex **1**, although the effects should be somewhat attenuated.

To test this experimentally, electrochemical studies on the OsO_4−pyridine systems were performed. The one-electron reduction potential of osmium tetroxide in the presence of a series of substituted pyridines was measured by cyclic voltammetry. Reversible cyclic voltammograms were obtained at a platinum wire electrode in methylene chloride using 0.65 M tetrabutylamonium tetrafluoroborate ($Bu_4N^+BF_4^-$) as the electrolyte at room temperature. The ferrocene/ferrocenium couple (307 mV vs SCE)[36] was used as the reference. Under these conditions only one reversible osmium couple was observed while two species, OsO_4 and OsO_4−L (where L = tertiary amine ligand), were present in solution. The measured potentials should vary with amine concentration according to the equation

$$E^\circ = E_f^\circ + \frac{RT}{aF} \ln \frac{(1 + K_{eq}^{-}[L])}{(1 + K_{eq}[L])} \qquad (2)$$

where E° is the standard potential for the couple

(36) Gagné, R. P.; Koval, C. A.; Lisensky, G. C. *Inorg. Chem.* **1980**, *19*, 2854.

$$\langle [OsO_4], [OsO_4{-}L] \rangle + e^- \rightleftharpoons \langle [OsO_4]^-, [OsO_4{-}L]^- \rangle \quad (3)$$

E_f° is the standard potential for the OsO_4/OsO_4^- couple, K_{eq} is the formation constant for the $[OsO_4{-}L]$ complex, and K_{eq}^- is the formation constant for the reduced complex, $[OsO_4{-}L]^-$ (*a* and *F* are constants). As the ligand concentration is increased so that K_{eq} [L] and K_{eq}^- [L] $\gg$ 1, eq 2 simplifies to eq 4 where E_c° is the standard potential for the $[OsO_4{-}L]$ complexes. As

$$E_c^\circ = E_f^\circ + \frac{RT}{aF} \ln(K_{eq}^-/K_{eq}) \quad (4)$$

with the comparison of rate constants for the series of styrene osmylations using differently substituted pyridines, a comparison of the reduction potentials for solutions containing OsO_4 and a ligand must account for the fast and reversible equilibrium that occurs. The reduction potentials of the solutions should reach a maximum value at some concentration of the ligand. Experimentally these maximum values of the reduction potentials could not be achieved because of limited ligand solubility and contamination of the electrode. Figure 4 clearly shows, however, that the reduction potentials approached an asymptote. A limiting potential was observed only in the case of pyridine where the reduction potential in neat amine was identical to that measured in 2 M pyridine (−165 mV vs SCE). A qualitative correlation between the Hammett σ constant for the pyridine substituents and the reduction potentials is also evident from Figure 4. Free OsO_4, with a reduction potential of −60 mV,[37] is more easily reduced than any of the amine−OsO_4 complexes, which become more difficult to reduce as the basicity of the amine increases.

To investigate the influence of the remote substituents on the structural properties of the OsO_4−ligand complexes, X-ray crystal structures were obtained for three different pyridine complexes. Each of the 18-electron complexes was crystallized by vapor-phase diffusion of pentane into toluene solutions of OsO_4 and the amine. ORTEP depictions of osmium tetroxide complexes with 4-pyrrolidinopyridine (**2**), 4-phenylpyridine (**3**), and 4-cyanopyridine (**4**) are shown in Figure 5. In each case the geometry at the metal is distorted trigonal bipyramidal, but the length of the nitrogen−osmium(VIII) dative bond is influenced significantly by the substituent on the pyridine ring. The N−Os bond length of the 4-pyrrolidinopyridine complex is more than 0.13 Å shorter than the corresponding bond length for the 4-cyanopyridine complex (2.318 Å vs 2.452 Å, respectively). The crystal structure for the quinuclidine−OsO_4 complex has been reported previously, and the N−Os bond length in this complex is 2.37 Å.[23a] A N−Os bond length of 2.49 Å, determined from the crystal structure of the complex between OsO_4 and the first-generation alkaloid ligand 9-*O*-(dimethylcarbamoyl)dihydroquinidine, was also reported previously.[24] The bond length in the alkaloid complex seems longer than expected based on the equilibrium constant for this ligand. The hindered steric environment around the alkaloid's quinuclidine moiety provides a likely explanation for this effect.

In summary, the reduction potentials of the amine−OsO_4 complexes correlate directly with basicity of the amine. Complexes of type **1** where the amines are strongly basic and therefore have large equilibrium constants favoring coordination to OsO_4, are more difficult to reduce than their analogs formed from weakly basic and poorly binding amines. No clear correlation exists, however, between the amine's basicity and the structural features of complex **1**. In the substituted pyridine complexes a definite shortening of the N−Os bond occurs as the basicity of the amine increases, but this trend does not extend to the quinuclidine−OsO_4 complex. The minute structural variations in the amine−OsO_4 complexes are not as significant as the direct correlation between the K_{eq} values and the reduction potentials of these species.[38]

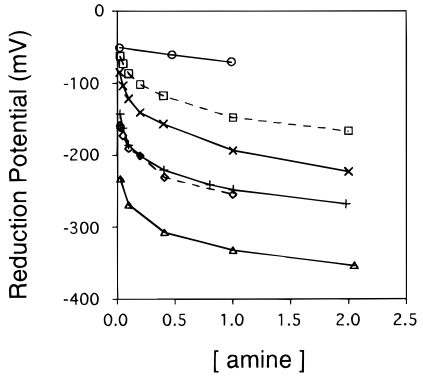

Figure 4. Plot of one-electron reduction potentials of solutions containing amine ligands/OsO_4 vs ligand concentrations (○ = 4-cyanopyridine, □ = pyridine, × = tetrahydroisoquinoline, + = 4-*N*,*N*-dimethylaminopyridine, ◇ = 4-pyrrolidinopyridine, △ = quinuclidine).

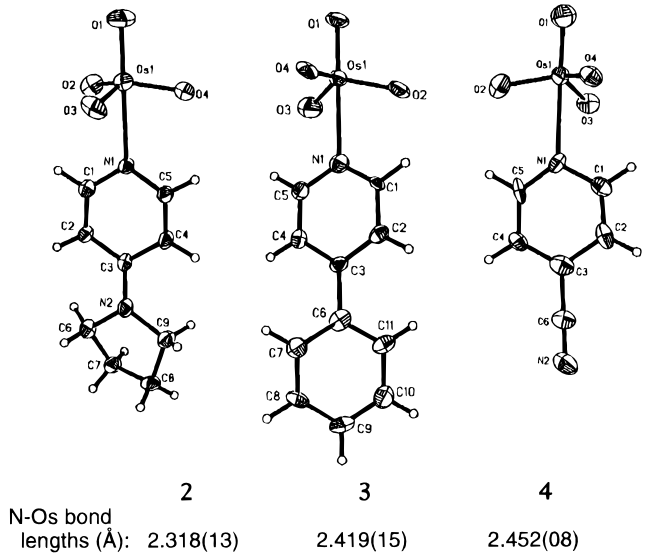

Figure 5. ORTEP depictions of the X-ray crystal structures of 4-pyrrolidinopyridine−OsO_4 (**2**), 4-phenylpyridine−OsO_4 (**3**), and 4-cyanopyridine−OsO_4 (**4**).

Hammett Studies To Determine the Influence of Substrate Substituents in Osmylations of Monosubstituted Alkenes. Because of the inherent difficulties in comparing reactivity across a series of related amine−OsO_4 complexes, a different type of Hammett study was undertaken. The influence of substituents on the substrate was investigated by monitoring the rates of osmylation of a series of substituted styrenes. Initially, pyridine-accelerated osmylations were investigated. These reactions were performed under pseudo-first-order conditions with limiting OsO_4 in toluene at 25.0 °C. An excess of the styrene (20 equiv) was used, and the concentration of the pyridine was varied to establish that the usual pattern of rate saturation at high ligand concentrations was followed. The reaction rates were measured by monitoring the formation of the bis(pyridine)osmium(VI) glycolate by UV−visible spectroscopy (300−320 nm) or by monitoring the rate of disappearance of the amine−OsO_4 complex. Several of the pyridine−

(37) Wallis, J. M.; Kochi, J. K. *J. Am. Chem. Soc.* **1988**, *110*, 8207.

(38) For additional studies attempting to correlate different features of amine-accelerated osmylations, see: Kwong, H.-L. Ph.D. Thesis, Massachusetts Institute of Technology, 1993.

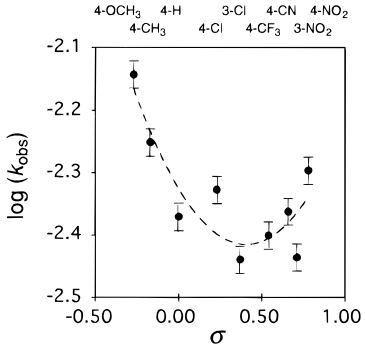

Figure 6. Nonlinear Hammett plot based on the pseudo-first-order rate constants of Scheme 3 ($[OsO_4]_o = 2.00 \times 10^{-4}$ M, $[\text{styrene}]_o = 4.00 \times 10^{-3}$ M, $[\text{py}]_o = 1.25 \times 10^{-1}$ M).

Scheme 3

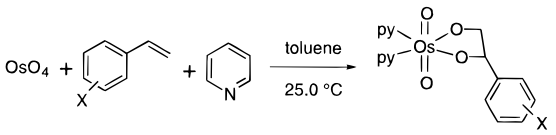

glycolate complexes were isolated and characterized to insure that the measured kinetics derived from the appropriate reaction (Scheme 3).

A plot of the logarithm of the observed absolute rate constants at a constant pyridine concentration (0.125 M) vs the σ parameters (Figure 6) of the styrene substituents was prepared to determine if a linear free energy relationship (LFER) was obeyed. An unusual pattern was observed. The pyridine-accelerated reactions were faster for styrenes bearing either electron-donating or electron-withdrawing substituents on the aromatic ring. The distinctly curved Hammett plot obtained under these specific reaction conditions exhibited a minimum near the point corresponding to 3-chlorostyrene.[39] The electronic effects observed in the osmylations of these styrenes are relatively small. The fastest and slowest absolute rate constants for the reaction series corresponding to Figure 6 differ by only a factor of 2. This indicates a very weak substituent effect consistent with a mechanism having negligible charge separation. Both the concerted "[3 + 2]" mechanism and the stepwise pathway via the osmaoxetane should proceed with little or no charge development in the transition state. The approximately parabolic Hammett study using pyridine to accelerate the osmylations of styrenes provides an intriguing clue about the transition state of the rate-determining step.

The study of substrate substituent effects was extended to include osmylation reactions accelerated by other substituted pyridines having markedly different basicities and capacities to coordinate to OsO_4. Figure 7 represents a summary of these data. Distinctly different Hammett relationships were observed for each reaction series, and several characteristics of the plots require comment. Most importantly, all of the individual Hammett plots for these amine-accelerated osmylations are nonlinear. Each of the curved Hammett plots in Figure 7 exhibits an approximate minimum corresponding to the least reactive styrene. The positions of the minima vary in a systematic fashion and these points correspond to more electron-withdrawing (or less electron-donating) substituents on styrene as the basicity (and binding constant) of the pyridine decreases. As a result, the osmylation of styrenes accelerated by 4-pyrrolidinopyridine appears to be dominated by a process with a positive ρ value, while the 4-cyanopyridine-accelerated series appears to be dominated by a process with a negative ρ value.

(39) The data in Figure 6 correlated very poorly ($r = 0.65$) with a linear least-squares fit. The second-order polynomial fit shown provided a much better correlation ($r = 0.89$) although this is only an indication of nonlinearity and has no physical significance.

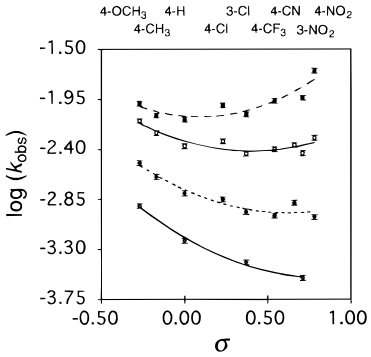

Figure 7. Combined Hammett plots based on the measured pseudo-first-order rate constants for osmylations of substituted styrenes (● = 4-pyrrolidinopyridine, ○ = pyridine, ◆ = 4-cyanopyridine, ◇ = 3,5-dichloropyridine; $[OsO_4]_o = 2.00 \times 10^{-4}$ M, $[\text{styrene}]_o = 4.00 \times 10^{-3}$ M, $[\text{pyridine}]_o = 1.25 \times 10^{-1}$ M).

The inclusion of several different Hammett studies in Figure 7 diminishes the apparent degree of curvature in the plot due to compression of the scale of the ordinate. The Hammett plot for the pyridine-accelerated reactions from Figure 6 is included in Figure 7 to illustrate this effect. A Hammett plot based on the kinetics of the osmylation of substituted styrenes *in the absence of amine ligands* was conducted to complement the study summarized in Figure 7 (Supporting Information). The rates of these unaccelerated osmylations in toluene at 25 °C exhibit a linear Hammett relationship ($r = 0.99$) with a ρ value of -0.9 for an abbreviated range of substrates. The data for the unaccelerated osmylation series agree closely with observations made by Henbest for unaccelerated osmylations of symmetrically substituted *trans*-stilbenes.[16]

All of the reactions used for the analysis in Figure 7 employed the pyridine ligands at 0.125 M concentrations. For the strongly coordinating pyridines (e.g., 4-pyrrolidinopyridine and DMAP), the experimental rate constants obtained under these conditions were within 5% of the ceiling rates, and the shape of the Hammett plot did not change when the extrapolated k_c values were used. The experimental rate data for osmylations accelerated by the poorly binding ligand 4-cyanopyridine were only at $\leq$50% of the saturation rates. The shape of the Hammett plot based on the extrapolated k_c values for these reactions also has approximately the same shape.

The influence of amine concentration on the degree of curvature in the Hammett plots for osmylations was investigated by using the moderately binding ligand 4-picoline to accelerate styrene osmylations in acetonitrile. Hammett studies at several different concentrations of 4-picoline were performed. Selected results are graphically summarized in the form of a combined Hammett plot (Figure 8). As part of this study, a linear Hammett plot was determined for the unaccelerated osmylations of styrene in acetonitrile. A ρ value of -0.7 was determined for these osmylations in the absence of any coordinating tertiary amine, and this is in accord with the observations made for the same reaction series in toluene (vide supra). The data in Figure 8 show that a distinct change in the curvature of the Hammett plots occurs as the concentration of the amine decreases. The change in the curvature of the Hammett plot in response to different concentrations of amine indicates that the rate-determining step in osmylations is not uniform even within a closely related series of reactions. This implicates the participation of at least two distinct mechanisms for the amine-accelerated reactions in addition to the mechanism when no

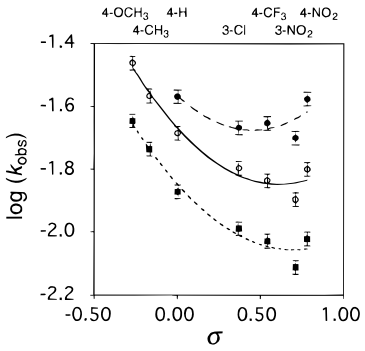

Figure 8. Hammett plots based on the observed pseudo-first-order rate constants of the 4-picoline accelerated osmylations of substituted styrenes in acetonitrile at 25.0 °C ($[OsO_4]_o = 2.00 \times 10^{-4}$ M, $[styrene]_o = 4.00 \times 10^{-3}$ M, [4-picoline]$_o$ = 1.75 M, -●-; 2.5×10^{-1} M, -○-; 2.5×10^{-2} M, -■-).

Scheme 4

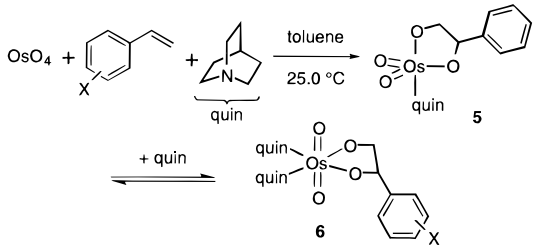

amine is involved. Competition between the accelerated and unaccelerated reactions as the source of the change in Hammett plot curvature can be ruled out because the rates of the accelerated reactions used for Figure 8 are at least 100 times faster than the rates for the unaccelerated osmylations.[40] To avoid the potential pitfalls of reaching a general mechanistic conclusion based on the data from osmylations of a single type of alkene accelerated only by pyridines, stoichiometric osmylations using other tertiary amine ligands were analyzed.

The simplest approach to determining the generality of the unusual substrate electronic effects involved using quinuclidine and modified alkaloid ligands to accelerate the osmylation of styrenes. Quinuclidine presents a more hindered coordination site than the relatively flat pyridine derivatives, and the alkaloid ligands provide an extremely complex steric environment near the coordinating nitrogen. The osmium(VI) glycolates formed in the presence of quinuclidine may have either one or two coordinated quinuclidines depending on the concentration of the amine (Scheme 4).[41] The monoquinuclidine complex **5** exhibits a broad absorbance between 600 and 750 nm in the UV−visible spectrum, and the rate of osmylation can be measured by monitoring the rate of increase of this absorbance when low to moderate concentrations of quinuclidine are present. At higher concentrations of the amine, the absorbance of complex **5** is almost totally suppressed due to formation of **6**, and the rate of osmylation must be determined by measuring the disappearance of the quinuclidine−OsO_4 complex. The rates measured in either way are identical, and this shows that quinuclidine-accelerated osmylations are at ligand saturation even for small excesses (∼10 equiv) of quinuclidine.

A Hammett plot based on the rates of quinuclidine-accelerated osmylations also displayed a curved shape with a distinct minimum (Figure 9). The data from this Hammett study show

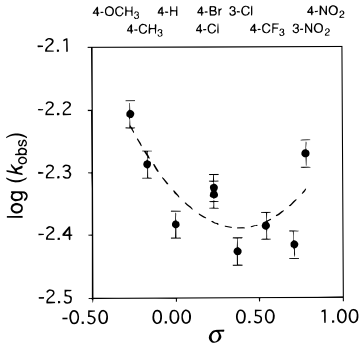

Figure 9. Hammett plot based on the observed pseudo-first-order rate constants for the quinuclidine-accelerated osmylation of substituted styrenes in toluene at 25 °C ($[OsO_4]_o = 2.00 \times 10^{-4}$ M, $[styrene]_o = 4.00 \times 10^{-3}$ M, [quinuclidine]$_o$ = 1.25×10^{-1} M).

that the nonlinear relationship between rate and the substituent parameters is *neither* an artifact arising from comparison of reaction series at different points on the saturation curves nor a phenomenon specific to pyridine-accelerated reactions. Due to the curvature in the Hammett plot a ρ value cannot be calculated directly. The position of the approximate minimum in Figure 9 corresponds to 3-chlorostyrene. The location of the minimum is very similar to that observed in the pyridine-accelerated series (Figure 6), and the magnitude of the ligand acceleration is nearly identical to that observed in the unsubstituted pyridine series. This similarity in the response to substrate substituents is remarkable considering the disparity in the equilibrium constants for the two amines.

The amines used in the Hammett studies to this point have been sterically uncomplicated. The substituted pyridines differed only in their basicity and capacity to coordinate to OsO_4. Quinuclidine is sterically more bulky than pyridine, and this manifests itself in the relatively small equilibrium constant for the coordination of the second quinuclidine to the Os(VI) glycolate (Scheme 4). In both cases, interactions between the amine and the substrate should be minimal. A Hammett study using DHQD-CLB to accelerate the osmylation of substituted styrenes was performed to determine substrate substituent effects in systems where noncovalent interactions between the ligand and substrate exist and asymmetric induction occurs. The interactions of the alkaloid ligands π-electrons with the substrate results in enormous rate accelerations, particularly for alkenes bearing aryl groups.[2c] The steric environment near the nitrogen of the quinuclidine moiety in alkaloids significantly reduces the equilibrium constant for coordination to OsO_4, so these amines represent another extreme in reactivity. Of greatest interest to synthetic organic chemists are the second-generation bisalkaloid ligands such as PHAL,[42] PYR,[43] DPP,[44] and AQN[45] due to the higher enantioselectivity achieved with these ligands in the catalytic AD. The relatively simple ligand DHQD-CLB suffices for the purpose of investigating the generality of the unusual Hammett behavior in stoichiometric osmylations.

Previous work has shown that the osmium(VI) glycolates obtained using first-generation ligands have only a single bound alkaloid.[46] The absolute rates of osmylation were measured by

(40) For a discussion of Ligand Accelerated Catalysis, see: Berrisford, D. J.; Bolm, C.; Sharpless, K. B. *Angew. Chem., Int. Ed. Engl.* **1995**, *34*, 1059.38.

(41) Schröder, M.; Nielson, A. J.; Griffith, W. P. *J. Chem. Soc., Dalton Trans.* **1979**, 1607.

(42) Sharpless, K. B.; Amberg, W.; Bennani, Y. L.; Crispino, G A.; Hartung, J.; Jeong, K.-Y.; Kwong, H.-L.; Morikawa, K.; Wang, Z.-M.; Xu, D.; Zhang, X.-L. *J. Org. Chem.* **1992**, *57*, 2768.

(43) Crispino, G. A.; Jeong, K.-S.; Kolb, H. C.; Wang, Z.-M.; Xu, D.; Sharpless, K. B. *J. Org. Chem.* **1993**, *58*, 3785.

(44) Becker, H.; King, S. B.; Taniguchi,M.; Vanhessche, K. P. M.; Sharpless, K. B. *J. Org. Chem.* **1995**, *60*, 2940.

(45) Becker, H.; Sharpless, K. B. *Angew. Chem., Int. Ed. Engl.* **1996**, *35*, 448.

(46) Pearlstein, R. M.; Blackburn, B. K.; Davis, W. M.; Sharpless, K. B. *Angew. Chem., Int. Ed. Engl.* **1990**, *55*, 766.

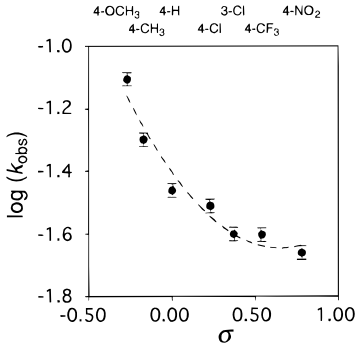

Figure 10. Hammett plot based on the observed rate constants in the DHQD-CLB-accelerated osmylations of substituted styrenes in toluene at 25 °C ($[OsO_4]_o = 2.00 \times 10^{-4}$ M, $[\text{styrene}]_o = 4.00 \times 10^{-3}$ M, $[\text{DHQD-CLB}]_o = 5.00 \times 10^{-2}$ M).

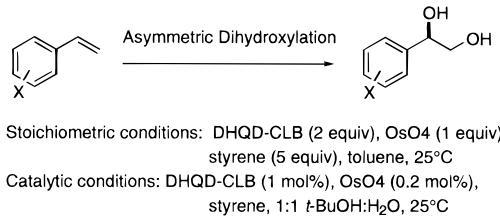

Figure 11. Preparative AD reactions used to investigate the influence of remote substituents on facial selectivity.

monitoring the absorbance of this complex at 685 nm in the UV−visible spectrum. The Hammett plot obtained using DHQD-CLB to accelerate the osmylation of styrenes in toluene at 25.0 °C exhibits modest curvature (Figure 10). The observed reaction rates change less as the substituent on the styrene becomes more electron-withdrawing, but a distinct minimum does not exist. The extent of curvature in the Hammett plot parallels that observed in the Hammett plots of osmylations accelerated by the poorly binding pyridine derivatives (Figure 7). This similarity is remarkable considering the fact that the rate accelerations caused by DHQD-CLB are substantially greater than those obtained using either 4-cyano- or 3,5-dichloropyridine. The Ligand Acceleration Effect (LAE) values[40] for DHQD-CLB range from 10^2-10^3, whereas the LAE for 4-cyanopyridine ranges from 5−10.

The inclusion of a Hammett study employing an optically active alkaloid ligand to accelerate stoichiometric osmylations raises the issue of electronic effects in asymmetric induction. To address this, both stoichiometric and catalytic AD reactions were performed on a preparative scale with the styrenes used in the kinetic Hammett study (Figure 11). The catalytic reactions were run under the standard conditions recommended for monosubstituted alkenes.[1] The concentrations of osmium and ligand in the organic phase of the catalytic reaction are difficult to assess,[47] but the *maximum* values are $[OsO_4] = 2 \times 10^{-4}$ M and $[\text{DHQD-CLB}] = 1 \times 10^{-3}$ M. For the stoichiometric variant, the initial concentrations were $[OsO4]_o = 4.2 \times 10^{-2}$ M and $[\text{DHQD-CLB}]_o = 8.5 \times 10^{-2}$ M.

The enantioselectivities for these reactions are depicted graphically in Figure 12. The data for the stoichiometric AD reactions in toluene show that remote electronic substituents definitely influence facial selectivity, and the pattern parallels the kinetic behavior. Higher enantioselectivity was obtained with styrenes bearing electron-donating substituents, and electron-withdrawing groups on the styrene resulted in poorer facial selectivity. The same general behavior was determined for the

(47) Ogino, Y.; Chen, H.; Kwong, H.-L.; Sharpless, K. B. *Tetrahedron Lett.* **1991**, *32*, 3965.

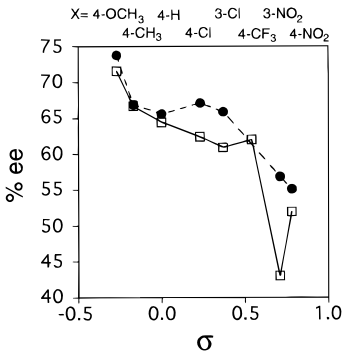

Figure 12. The influence of styrene substituents on enantioselectivity in stoichiometric (-●-) and catalytic (-□-) variants of the AD reaction (Figure 11).

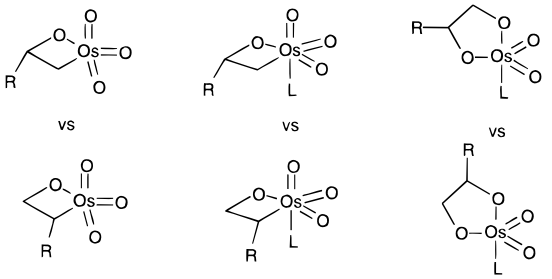

Figure 13. Possible regioisomers in the osmylation of monosubstituted alkenes.

catalytic AD. The differences in the concentrations of ligand and OsO_4 and the differences in solvent polarity, factors that dramatically influence the equilibrium for ligand−OsO_4 complexation, did not alter the overall trend in asymmetric induction. The erosion of enantioselectivity and corresponding decrease in the rates of alkaloid-accelerated osmylation observed as the styrene substituent becomes more electron-withdrawing probably results from a decrease in the noncovalent interactions between the aromatic group of the substrate and the binding pocket of the ligand.

Hammett Studies Employing Di- and Trisubstituted Alkenes. The set of Hammett studies described above is not sufficient for a study of osmylation reactions because an unusual response to substituents could result from a change in the regiochemistry of intermediate and/or product formation. For example, two regioisomers of an osmaoxetane intermediate, and its ligated counterpart, may form in reactions with monosubstituted alkenes (Figure 13). A similar regiochemical argument may be made for the transition state in the proposed "[3 + 2]" pathway. The preference for formation of any of these regioisomers may change in response to electronic perturbations, and it is necessary to determine whether nonlinear Hammett relationships are observed in systems where such regiochemical issues are not relevant.

The use of symmetrically substituted *trans*-stilbenes in stoichiometric reactions with OsO_4 and different amine ligands provides the most direct experimental method to determine the role of regioisomerism in an intermediate or transition state. Hammett studies employing substituted *trans*-stilbenes as substrates and three different amines (DMAP, quinuclidine, and DHQD-CLB) were conducted under conditions similar to those used for the styrene reactions. All reactions in a related series used identical concentrations of OsO_4, substrate, and ligand. Although substituent parameters are considered additive,[27] each of the Hammett plots based on symmetrically substituted *trans*-stilbenes uses σ values corresponding to only a single substituent. No ρ values were calculated because curvature was observed in each of the plots, so the omission of a factor of 2

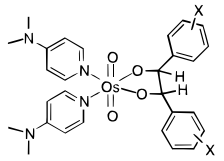

7

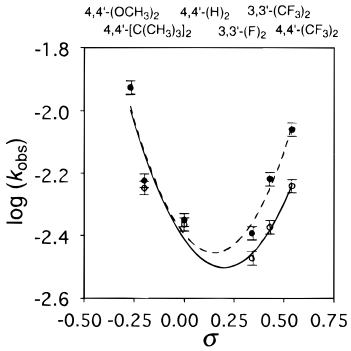

Figure 14. Hammett plots based on the pseudo-first-order rate constants of the DMAP-accelerated osmylations of *trans*-stilbenes in toluene at 25.0 °C ($[OsO_4]_o = 2.00 \times 10^{-4}$ M, $[\text{stilbene}]_o = 4.0 \times 10^{-3}$ M; $[\text{DMAP}]_o = 1.25 \times 10^{-1}$ M, -●- or 2.5×10^{-2} M, -○-).

in the scale of the *x*-axis does not alter the interpretation. The kinetics of the reactions were monitored by the standard spectrophotometric methods described above.

The same general trends that emerged from the Hammett relationships using styrenes were observed in the stilbene reactions. For the DMAP-accelerated osmylations where the product was the osmium(VI) glycolate having two coordinated amines (**7**), a markedly parabolic Hammett plot was obtained (Figure 14). The poor solubility of many *trans*-stilbenes and the corresponding glycolate complexes limited the number of substrates that could be used in these studies, but the range of substituents employed was large enough to provide mechanistically significant data. As in the case of the 4-picoline-accelerated styrene osmylations (Figure 8), the extent of curvature in the Hammett plot for DMAP-accelerated reactions of the stilbenes depended on the concentration of the amine. The influence of amine concentration was more pronounced for substrates bearing electron-withdrawing substituents. These data clearly show that the unusual response to substrate substituent effects is a general characteristic of osmylation reactions in the presence of strongly coordinating tertiary amines.

The investigation of substituent effects using *trans*-stilbenes was extended to include osmylations accelerated by quinuclidine and DHQD-CLB. The Hammett plot for the quinuclidine-accelerated series in toluene is depicted in Figure 15. A modest amount of curvature was observed in the quinuclidine series, and an approximate minimum corresponding to the rate of 3,3′-difluorostilbene exists. The measured rates of reaction for the quinuclidine series did not depend on the concentration of the amine indicating that ligand saturation had been achieved. A comparison of the kinetic data and Hammett plots of the DMAP-stilbene series vs the Hammett plot of the quinuclidine-stilbene series reveals the same patterns that were observed in the 4-pyrrolidinopyridine-styrene and quinuclidine-styrene series. Large excesses of the electron-rich pyridine ligands afforded more ligand acceleration than that observed with the more strongly coordinating quinuclidine. Also, the minima in the Hammett plots for the quinuclidine reactions corresponded to more electron-poor substrates.

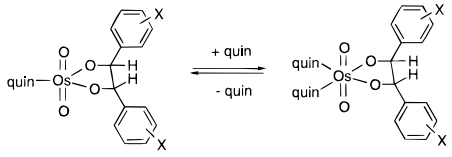

8 **9**

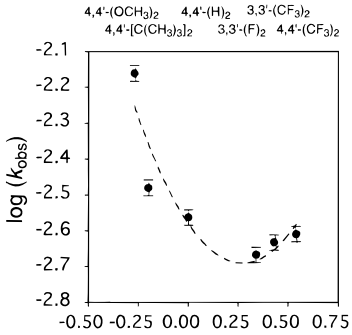

Figure 15. Hammett plot based on the absolute rates constants of the stoichiometric quinuclidine-accelerated osmylations of *trans*-stilbenes in toluene at 25.0 °C ($[OsO_4]_o = 2.00 \times 10^{-4}$ M, $[\text{stilbene}]_o = 4.0 \times 10^{-3}$ M; $[\text{quinuclidine}]_o = 1.25 \times 10^{-1}$ M.

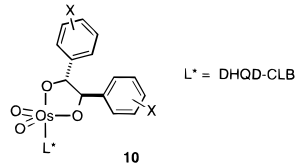

10

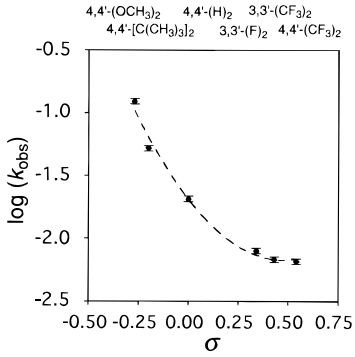

Figure 16. Hammett plot based on the rate constants of the DHQD-CLB-accelerated osmylations of stilbenes in toluene at 25.0 °C ($[OsO_4]_o = 2.00 \times 10^{-4}$ M, $[\text{stilbene}]_o = 4.0 \times 10^{-3}$ M; $[\text{DHQD-CLB}]_o = 1.25 \times 10^{-1}$ M).

Figure 16 shows the Hammett plot based on the measured kinetics for the formation of complex **10** in the DHQD-CLB-accelerated osmylations of the stilbenes. Similar to the DHQD-CLB/styrene series, a nearly linear correlation existed between the logarithm of the observed rate constant and the substituent parameter. A least squares linear fit of the Hammett plot afforded a moderate correlation ($r = 0.96$), and a ρ value of -1.5 can be calculated. This simplified analysis is misleading unless Figure 16 is considered in the context of the Hammett plots for the other amine-accelerated reaction series. The Hammett plot is clearly nonlinear, but the amount of curvature is very small. The difference in rate extremes for the DHQD-CLB-accelerated osmylations was greater, in part, because of the smaller degree of curvature. The enantioselectivity of the symmetric stilbene series was not determined, but alkaloid ligands afford stilbene diols of much higher enantiomeric excess than comparable styrene diols.[1]

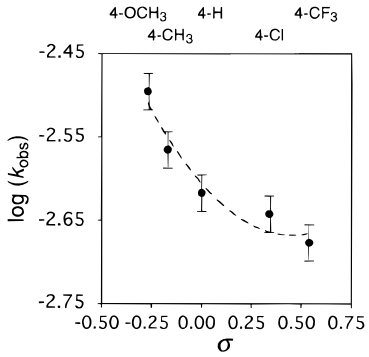

Figure 17. Hammett plot based on the rate constants of the DHQD-CLB-accelerated osmylations of triphenylethylenes (**11**) in acetonitrile at 25.0 °C ($[OsO_4]_o = 2.00 \times 10^{-4}$ M, [triphenylethylene]$_o = 4.0 \times 10^{-3}$ M; [DHQD-CLB]$_o = 1.25 \times 10^{-1}$ M).

One final set of Hammett studies was performed. The investigation of substituent effects for structurally different alkenes was extended to include triphenylethylenes (**11**) bearing substituents at the para position of the C(2) phenyl moiety. The osmylations of these bulky trisubstituted alkenes represent an extreme in terms of the steric interactions between ligand, substrate, and OsO_4. This is particularly important if the coordinating amine is an alkaloid ligand. If an osmaoxetane

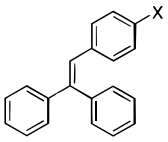

11

intermediate is involved, then the regioisomer with the osmium bound to the carbon with only one aromatic group should predominate. Substituents on the phenyl group of the carbon directly involved in the proposed migration from the osmium to an oxo group in the transition state may provide insight into the nature of this step.

The study of substrate electronic effects on the rate of osmylation was brought to a close by investigating the kinetics of the DHQD-CLB-accelerated osmylations of the triphenylethylene derivatives. This reaction series exhibits a very weak substrate electronic effect. The difference in reaction rates from the most electron-donating substituent to the strongest electron-withdrawing one is less than a factor of 2, even using large excesses of the ligand (625 equiv based on limiting OsO_4). The shape of the Hammett plot is indeterminate. A least-squares linear fit of the data afforded a poor correlation ($r = 0.92$), and a small ρ value of -0.2 for these data was determined. The slightly curved Hammett plot for the stoichiometric osmylations of the triphenylethylenes resembles the plots derived from the kinetics of the osmylations of styrenes (Figure 10) and stilbenes (Figure 16), and this is remarkable considering that only one of the phenyl groups in the triphenylethylenes bore substituents.

Discussion

The extensive body of data describing substituent effects in osmylation reactions collected in this study allows for a critical evaluation of the proposed mechanisms for the reaction of OsO_4 with alkenes. Electronic effects caused by remote substituents on the amine ligand can be difficult to interpret. The amine's substituent influences not only the equilibrium describing formation of the amine$-OsO_4$ complex (**1**) but also the reduction potential and structural features of this complex. In general, amines bearing electron-donating groups coordinate more strongly to OsO_4. The resulting 18-electron complexes have shorter N$-$Os bond lengths and higher reduction potentials than their counterparts with electron-withdrawing substituents. These effects were measured directly and are in accord with osmium tetroxide functioning as a Lewis acid toward the amine. However, anticipating the effects of electronically differentiated amines on the transition state of the osmylation process proved to be anything but straightforward.

For osmylations accelerated by the substituted-pyridine series, reaction rates decreased as the basicity of the pyridine decreased. Under identical experimental conditions, the differences in reactivity for strongly and weakly coordinating amines with nearly identical steric environments was often a factor of 10 or more. A comparison of the k_c values for these series revealed very small differences (only a factor of 2$-$3) between extremes. The negative ρ value calculated from the Hammett plot based on k_c values for substituted pyridine ligands (Table 2) is inconsistent with the positive ρ value obtained from the Hammett plot using saturation rates from substituted quinuclidine ligands (Table 3). In the case of the 4-substituted quinuclidine reactions, the more poorly binding amines afforded faster reaction rates than the parent compound. The pattern of ligand-acceleration in the quinuclidine series provides a strong argument against a simple concerted "[3 + 2]" mechanism (Figure 1). These data, however, do not provide unambiguous evidence for a stepwise mechanism.

Kinetic evaluation of substrate electronic effects in osmylations provided substantially more information about the mechanistic possibilities. The most striking feature of the present studies is the varied response of stoichiometric osmylation rates to substrate substituent effects. *All* of the Hammett plots for the amine-accelerated osmylations based on variation of the electronic properties of the alkenes exhibited some degree of curvature. The deviation from linearity in these free energy relationships appears to be related to the capacity of the amine to coordinate to osmium tetroxide. Strongly coordinating amines such as DMAP and quinuclidine afforded parabola-like Hammett plots, while poorly binding amines such as 4-cyanopyridine and DHQD-CLB caused only moderate curvature. The structure of the alkene (e.g., mono-, di-, or trisubstituted) influenced the nonlinear Hammett behavior, but no simple correlation between the substitution pattern/geometry of the alkene and electronic effects was apparent.

Failure to obey a linear free energy relationship based on empirical substituent parameters has been reported for several different types of reactions, and numerous explanations for this have been offered. An appreciable amount of scatter in the data can indicate that the particular set of substituent parameters (e.g., σ, σ^+, or σ^-) used for the attempted correlation is inappropriate for the extent and type of charge developing on the intermediate. The standard σ parameters afforded good linear correlations for the equilibria describing the substituted pyridine$-OsO_4$ complexation (Figure 2) as well as for the rates of unaccelerated osmylations in different solvents. These data, together with the fact that neither of the proposed mechanisms for amine-accelerated osmylations predict charge separation, indicate the suitability of the chosen parameters. In addition, the alternate substituent parameters did not yield linear free energy relationships.

A change in the reaction mechanism can also result in a nonlinear Hammett relationship. The hydrolysis of phenyl-substituted ethyl benzoate esters,[48] the solvolysis of 7-aryl-7-

(48) Leffler, J. E.; Greenwald, E. *Rates and Equilibria of Organic Reactions*; John Wiley & Sons: New York, 1963.

Scheme 5

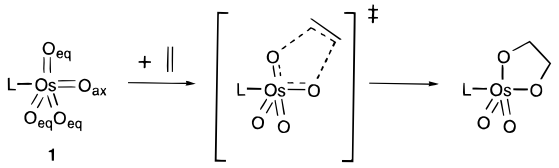

bicyclo[2.2.1]-hept-2-enyl derivatives,[49] and the solvolysis of 3-aryl-2-butylbrosylates[50] are well-known examples of reactions that exhibit nonlinear Hammett relationships caused by a change in mechanism. In these cases, the reactions involve positively charged intermediates that have different structures in response to the different substituents. The substituent effects determined in these classic studies are quite large, often corresponding to rate differences of several orders of magnitude. The fact that a change in mechanism can cause nonlinear Hammett behavior is very important from a theoretical perspective, regardless of the nature of the intermediate. To determine whether a change in mechanism can explain the curved Hammett plots observed for the charge-neutral osmylation reactions, it is necessary to consider the expected response to electronic effects in each of the proposed mechanisms.

The "[3 + 2]" Pathway. The concerted"[3 + 2]" pathway involving reaction of the amine−OsO_4 complex **1** at the axial oxygen and one of the equatorial oxygen atoms should resemble a 1,3-dipolar cycloaddition (Scheme 5). Another plausible explanation for nonlinear Hammett plots arose from mechanistic investigations of the cycloadditions of 1,3-dipoles with alkenes. Several examples of nonlinear Hammett relationships have been observed for 1,3-dipolar additions to unsaturated compounds.[51] Firestone argued that the unusual response to electronic substituents occurred because the dipolar cycloadditions proceeded via a nonspin-paired intermediate having biradical character.[52] According to this model, any substituent adjacent to the sites with radical character should result in faster rates. Also implicit in this model is that collapse of the 1,5-biradical intermediate must occur more rapidly than rotation about single bonds. The extremely high stereospecificity in the additions of 1,3-dipoles to alkenes and the failure to observe any products that could unambiguously be attributed to a radical process are often cited as evidence against Firestone's mechanistic proposal. Computational and theoretical studies indicate that certain 1,3-dipoles have a substantial amount of diradical character as opposed to zwitterionic character, but this does not necessarily imply reaction via a discrete diradical intermediate.[53]

A far more general and satisfactory rationale for the unusual Hammett relationships observed in 1,3-dipolar cycloadditions has been developed. Sustmann proposed a frontier molecular orbital (FMO) model based on the classical, pericyclic cycloaddition mechanism that can adequately explain the Hammett phenomena in these reactions.[54,55] According to this FMO model, the dipole-dipolariphile HOMO−LUMO energy differences dictate the energy of the transition state (Figure 18). The critical interactions are directly proportional to the sum of the reciprocals of energy differences (eq 5). Of course eq 5 represents a simplification, and terms accounting for closed-shell repulsions, coulombic and charge-transfer interactions, and differences in HOMO−LUMO overlap have been omitted. Application of this model allows 1,3-dipole cycloadditions to be organized into three distinct categories based on the relative energies of the molecular orbitals of the reaction partners. Type I dipolar cycloadditions occur with dipoles having relatively high HOMO and LUMO energies compared to the dipolariphile ($E_I < E_{II}$). These cycloadditions should be accelerated by electron-donating substituents on the dipole and electron-withdrawing substituents on the dipolariphile. Substitution on either reactant will cause the terms ΔE_I and ΔE_{II} to be affixed to the denominators in eq 5, and an example of the change in the relevant orbital energies caused by a substituent on the dipolariphile is shown in Figure 18. Conversely, type III cycloadditions arise when the orbital energies of the dipolariphile are higher than those of the dipole ($E_I > E_{II}$), and these cycloadditions should be accelerated by electron-withdrawing substituents on the dipole and electron-donating substituents on the dipolariphile. Linear Hammett relationships are expected for both type I and type III reactions although the ρ values will be of opposite sign. The most unusual type of dipolar addition, type II, occurs when the HOMOs and LUMOs of both dipole and dipolariphile are of roughly equal energy ($E_I \sim E_{II}$). Any type of electron-donating or electron-withdrawing substituent on either reactant accelerates the reaction. Ideally, type II cycloadditions will result in parabolic Hammett plots.

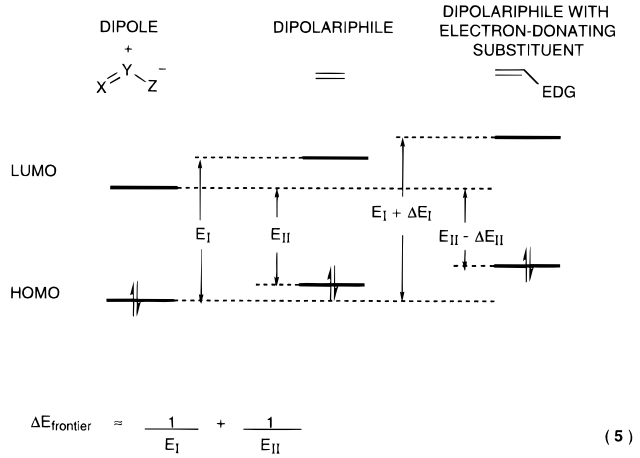

$$\Delta E_{frontier} \approx \frac{1}{E_I} + \frac{1}{E_{II}} \quad (5)$$

Figure 18. Frontier molecular orbital interactions proposed to dictate the energy of the transition state in 1,3-dipolar cycloadditions.

The logic of the FMO model advocated by Huisgen and Sustmann and the ample body of experimental and computational[56] evidence that supports it make it appealing to try to evaluate the Hammett studies in osmylations using a similar model. For the pyridine-accelerated osmylations of substituted styrenes summarized in Figure 6, the approximately parabolic shape of the Hammett plot is consistent with the behavior of a type II 1,3-dipolar cycloaddition. The substituted pyridine-accelerated osmylations summarized in Figure 7 exhibit a systematic transition in the degree of curvature of the Hammett plots that is consistent with a gradual change in the behavior of the reactions from type I to type III cycloadditions as the binding constant of the amine decreases.

(49) Gassman, P. G.; Fentiman, A. F., Jr. *J. Am. Chem. Soc.* **1970**, *92*, 2549.

(50) Brown, H, C.; Kim, C. J.; Lancelot, C. J.; Schleyer, P. v. R. *J. Am. Chem. Soc.* **1970**, *92*, 5244.

(51) (a) Dondoni, A. *Tetrahedron Lett.* **1967**, 2397. (b) Battaglia, Dondoni, A. *Ric. Scient.* **1968**, *38*, 201. (c) Bast, K.; Christl, M.; Huisgen, R.; Mack, W. *Chem. Ber.* **1973**, *106*, 3312. (d) Eckell, A.; George, M. W.; Huisgen, R.; Kende, A. S. *Chem. Ber.* **1977**, *110*, 578.

(52) (a) Firestone, R. A. *J. Org. Chem.* **1968**, *33*, 2285. (b) Firestone, R. A. *Tetrahedron* **1977**, *33*, 3009.

(53) Houk, K. N.; Yamaguchi, K. In *1,3-Dipolar Cycloaddition Reactions*; Padwa, A., Ed.; John Wiley & Sons: New York, 1984; Vol. 1, pp 407−450.

(54) Sustmann, R. *Tetrahedron Lett.* **1971**, 2721.

(55) Huisgen, R. In *1,3-Dipolar Cycloaddition Reactions*; Padwa, A., Ed.; John Wiley & Sons: New York, 1984; Vol. 1, pp 1−176.

(56) (a) Huisgen, R.; Fisera, L.; Giera, H.; Sustmann, R. *J. Am. Chem. Soc.* **1995**, *117*, 9671. (b) Sustmann, R.; Sicking, W.; Huisgen, R. *J. Am. Chem. Soc.* **1995**, *117*, 9679.

The data represented in Figure 7 could be used as an argument for the concerted "[3 + 2]" cycloaddition mechanism in amine-accelerated osmylations, but it is necessary to reevaluate this analysis. Numerous inconsistencies in the analogy between osmylation reactions and dipolar cycloadditions can be found in the Hammett studies reported here. A comparison of the Hammett plots for osmylations of structurally different alkenes (e.g., styrenes vs stilbenes) under identical conditions highlights the difficulty of explaining amine-accelerated osmylations using Sustmann's FMO theory. The position of the approximate minimum in a Hammett plot arising from a type II dipolar cycloaddition mechanism may be used to judge the suitability of the model.

The Hammett analysis of pyrrolidinopyridine-accelerated osmylations of styrenes in toluene (Figure 7) shows the parent styrene to be the least reactive of the series. The Hammett study based on DMAP-accelerated stilbene osmylations under identical conditions (Figure 14) has a minimum corresponding to a stilbene that is slightly more electron-poor than *trans*-stilbene. The FMO model predicts the opposite trend in the positions of the minima based on the very different ionization potentials (IPs) of the two alkenes. The IP for *trans*-stilbene is 7.7 eV, while the value for styrene is 8.4 eV.[57] Huisgen has shown that the IPs of dipolariphiles are directly proportional to the HOMO energies used in the FMO model.[55] Numerous other analyses of the reactivity of alkenes with nucleophilic and electrophilic reagents are also based on this assumption.[58] The substantial difference in the orbital energies of styrene and stilbene indicates it is unlikely that both will correspond to the minimum in Hammett plots with the same type II dipole. If styrene osmylation is postulated as the minimum in reactivity, the FMO model predicts that the stilbene osmylations should be approaching type III reactions with a minimum corresponding to a very electron-rich stilbene. The structural differences between stilbene and styrene may detract from this analysis, but Huisgen has shown that Sustmann's FMO model applies quite well to a series of dipolariphiles with dramatically different structures.[55]

Other inconsistencies can be noted between the observed Hammett relationships in amine-accelerated osmylations and those predicted by the Sustmann model for concerted cycloaddition reactions via **1**. A comparison of the positions of the minima in the Hammett plots for osmylation of the same alkenes using different ligands is particularly interesting. The Hammett plot for the 4-pyrrolidinopyridine-accelerated osmylations exhibits an approximate minimum corresponding to the rate of the parent styrene (Figure 7), while the quinuclidine-accelerated series (Figure 9) exhibits an approximate minimum corresponding to the rate of the more electron-deficient 3-chlorostyrene. The quinuclidine$-OsO_4$ complex should behave more like a type I dipole than the OsO_4 complex with 4-pyrrolidinopyridine, and the FMO model fails to explain the observed behavior. Several other examples of this type of reversal in Hammett behavior exist in the current studies. In addition, the measured rates of the quinuclidine-accelerated reactions, which are essentially identical to the ceiling rates, are slower than the rates corresponding to reactions using identical concentrations of DMAP. In the context of a mechanism similar to a 1,3-dipolar cycloaddition, these features are not reconcilable with either the different equilibrium constants for the two amines (K_{eq} $\sim$1800 M^{-1} for DMAP and $\sim$80 000 M^{-1} for quinuclidine)[59] or with the observed reduction potentials for their OsO_4 complexes (Figure 4).

The knowledge that tertiary amines accelerate osmylation reactions and form complexes of type **1** reversibly in solution could easily lead to the conclusion that **1** is the reactive intermediate. This premise for the ligand acceleration phenomenon is seriously challenged by the electrochemical studies presented here. The data in Figure 3 lead to a prediction of rate *deceleration* when amines are present. The slight change in geometry at osmium, from tetrahedral to distorted trigonal bipyramidal, that occurs upon complexation of the amine might force the oxo groups into a more reactive conformation. For ligand-acceleration to occur, however, the benefit derived from the structural change must more than compensate for the substantial increase in the LUMO energy. The different steric environments presented by pyridine and quinuclidine derivatives may also influence the reactivity of the intermediate(s) in the reaction. The crystal structures of the pyridine$-OsO_4$ complexes **2**, **3**, and **4** reveal some eclipsing between the pyridine ring and the equatorial oxo groups. The previously reported crystal structure of the quinuclidine$-OsO_4$ complex reveals that the quinuclidine moiety adopts a completely staggered conformation with respect to the equatorial oxo groups.[23] The influence of ligand topology and the significance of different extents of staggering in the these complexes is unknown. The effect of slight changes in the $O_{ax}-Os-O_{eq}$ angle in the various amine$-OsO_4$ complexes and differences in the N$-$Os bond lengths in complex **1** are equally difficult to interpret, especially in light of the apparent lack of correlation between these structural data, the equilibrium constants (K_{eq}), and the electrochemical reduction potentials in solution.

In summary, the analogy between the concerted "[3 + 2]" cycloaddition mechanism in amine-accelerated osmylations and 1,3-dipolar cycloadditions provides a possible, albeit tenuous, explanation for the unusual Hammett plots. The numerous inconsistencies between the observed kinetic behavior and that predicted by the FMO model coupled with the failure of this pathway to explain the inversion points in the modified Eyring plots[12] lead us now to consider the "[2 + 2]" mechanism.

The Stepwise "[2 + 2]" Pathway. A discussion of possible stepwise mechanisms in osmylations must first emphasize the difference between a concerted [2 + 2] cycloaddition mechanism (such as the $\pi_{2s} + \pi_{2a}$ interaction between two carbon$-$carbon double bonds) and the analogous process between metal$-$ligand multiple bonds and alkenes. In the latter case, an actual [2 + 2] step is thought not to be involved, and the designation "[2 + 2]" is only a formalism describing the overall formation of the four-membered osmaoxetane ring. The sequence by which the oxametallacycle is formed is proposed to require prior formation of an alkene$-$metal complex (**12**).[60]

The stepwise mechanism proposed for cinchona alkaloid-accelerated osmylation reactions is shown in Figure 19. Several important assumptions are implicit in this pathway, and it is helpful to highlight these. First, all of the equilibria preceding the irreversible rearrangement of ligated osmaoxetane **14** to the glycolate product are rapid and reversible under normal AD conditions. This condition is mandated by two facts: (1) the ligand accelerates the rate of reaction and (2) the acceleration effect reaches saturation at high ligand concentrations. If the microscopic rate constants leading to the metallaoxetane were decreased to the extent that one of them became rate-limiting, then the rate expression would change and the kinetic profile

(57) Streitweiser, A. *Molecular Orbital Theory for Organic Chemists*; John Wiley & Sons: New York, 1961.

(58) Freeman, F. *Chem. Rev.* **1975**, *75*, 439.

(59) K_{eq} for the binding of 4-pyrrolidinopyridine in toluene is expected to be $\sim$2500 M^{-1} based on extrapolation from the data in Table 1 and Figure 2.

(60) For a discussion of the interconversion olefin$-$methylidine complexes and metallacyclobutanes, see: Upton, T. H.; Rappé, A. K. *J. Am. Chem. Soc.* **1985**, *107*, 1206.

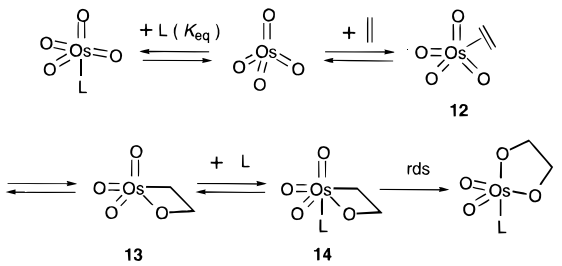

Figure 19. Component equilibria of the proposed stepwise "[2 + 2]" mechanism for the amine-accelerated osmylation of alkenes.

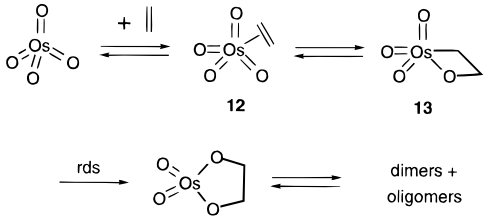

Figure 20. Proposed mechanism of osmylation in the absence tertiary amines.

with respect to amine concentration should also change. A discussion of the kinetic schemes corresponding to the general mechanism in Figure 19 under different limiting conditions has appeared in the literature.[61] None of the derived rate expressions for the various "[2 + 2]" pathways can adequately explain the range of Hammett behavior presented here.

It is presently not possible to obtain information about many of the component equilibria shown in Figure 19, but insight about the individual steps can be gained by consideration of related phenomena. The complexation of the alkene to the metal center in OsO_4 shown in Figure 19 is identical to the proposed mechanism of alkene osmylation in the *absence* of coordinating tertiary amines (Figure 20). The rate-determining step in the unaccelerated osmylation reactions should be migration of the carbon−osmium bond to an oxo group yielding the osmium(VI) glycolate. Dimerization of the 14-electron glycolate complexes then occurs rapidly.[62] The two Hammett studies of unaccelerated osmylations of substituted styrenes presented here (in toluene and in acetonitrile) reveal that the reaction pathway in the absence of coordinating amines responds in a straightforward manner to substituent effects. Both of these studies, as well as the earlier work by Henbest,[16] show that the unaccelerated reactions obey linear Hammett relationships with ρ values between −0.55 and −0.9. If these unaccelerated reactions proceed via the stepwise pathway, then migration of the carbon−osmium bond in the nonligated metallaoxetane intermediate (**13**) is faster with electron-releasing substituents and slower for electron-attracting substituents. By analogy with the equilibrium constants for the coordination of the substituted pyridines with OsO_4, the formation of the nonligated metallaoxetane **13** via an alkene−OsO_4 complex (**12**) should also exhibit a linear Hammett relationship with a negative ρ value of moderate magnitude.

The orbital interactions that govern the complexation of the alkene to OsO_4 and its subsequent oxo insertion to form the unligated osmaoxetane have not been investigated. Houk outlined six possible types of orbital interactions that could result in formal [2 + 2] adducts in the reactions of alkenes with ketenes based on geometry and extent of charge separation.[63] A parabolic reactivity plot was predicted for these net [2 + 2] additions when electron-donating and withdrawing substituents were placed on the reactants. The minimum in reactivity corresponded to the orbital controlled [2 + 2], which is thermally disallowed under the Woodward−Hoffman rules,[64] while faster reactivity was predicted for 1,4-diradicals or zwitterionic intermediates. A comparable analysis involving the formation of metallaoxetane intermediates from d^o transition metals and alkenes is not yet available, but calculations by Rappé and Goddard on reactions between alkenes and the metal−oxo functions in chromium(VI) complexes are certainly of interest.[65] Because the orbital description of the proposed formation of metallaoxetanes has not been clarified, it is important to note again that the designation "[2 + 2]" used for the stepwise mechanisms depicted in Figures 19 and 20 implies only the net formation of a metallaoxetane.[60]

Ample precedent for the rapid and reversible formation of four-membered metallacycles can be found in the olefin metathesis chemistry of metal alkylidene complexes.[66] Evidence for the rapid and reversible equilibria between metallaazetanes and their corresponding d^o metal−alkene complexes has been established for imido complexes of Ti, Zr, and V.[67] Reversible formation of an oxametallacyclobutene from a Ti(IV)-oxo group in the presence of a coordinating pyridine has recently been established, and formation of a stable metallaoxetane from Ti(IV) and an alkene has been accomplished.[68] Evidence of an analogous equilibrium for the formation of osmaoxetane intermediates remains elusive, however. Regardless of the uncertainty about whether the formation of the 16-electron osmaoxetane **13** should proceed with a negative ρ value, this step cannot be the rate-determining step with amine present because no ligand acceleration would occur. If the unaccelerated osmylations proceed via the stepwise mechanism, then the rate-determining step must be the migration of the carbon−osmium bond to form the 14-electron osmium(VI) glycolate (Figure 20). The Hammett studies for the unaccelerated reactions afford good linear correlations vs the substituent parameters, and the negative ρ values indicate that in the absence of coordinating amines this step is faster for electron-donating groups on the metallaoxetane. It is important to note that *nonlinear* Hammett plots with distinct minima have been observed in extrusions of *cis*-stilbenes from pentamethylcyclopentadienylrhenium(V) glycolates.[69] The microscopic reverse of this process has been proposed to be analogous to the mechanism of osmylation, and there is evidence implicating rhenaoxetane intermediates in the cycloreversion.[70] The parabolic Hammett plot determined for the rhenium(VI) glycolate extrusions is consistent with the parabolic Hammett plots reported here for amine-accelerated osmylations. Ring slippage of the pentamethylcyclopentadienyl ligand provides an intramolecular mimic of the extremely rapid and reversible equilibrium for coordination of the amine to osmium.

(61) Norrby, P.-O.; Gable, K. P. *J. Chem. Soc., Perkin Trans. 2* **1996**, 171.

(62) Casey, C. P. *J. Chem. Soc., Chem. Commun.* **1983**, 126.

(63) (a) Houk, K. N. *Acc. Chem. Res.* **1975**, *8*, 361. (b) Hall, J. K., Jr. *Angew. Chem., Int. Ed. Engl.* **1983**, *22*, 440.

(64) Woodward, R. B.; Hoffmann, R. *The Conservation of Orbital Symmetry*; Verlag Chemie: Weinheim, 1970.

(65) Rappé, A. K.; Goddard, W. A. III *J. Am. Chem. Soc.* **1982**, *104*, 448.

(66) For a review on the elucidation of the mechanism of olefin metathesis, see: Grubbs, R. H. In *Comprehensive Organometallic Chemistry*; Wilkinson, G., Ed.; Pergamon Press: Oxford, 1982; Vol 8, pp 499−552.

(67) Wigley, D. E. Prog. *Inorg. Chem.* **1994**, *42*, 239.

(68) Polse, J. L.; Andersen, R. A.; Bergman, R. G. *J. Am. Chem. Soc.* **1995**, *117*, 5393.

(69) Gable, K. O.; Juliette, J. J. J. *J. Am. Chem. Soc.* **1996**, *118*, 2625.

(70) (a) Gable, K. P.; Juliette, J. J. J. *J. Am. Chem. Soc.* **1995**, *117*, 955. (b) Gable, K. P.; Juliette, J. J. J.; Gartmann, M. A. *Organometallics* **1995**, *14*, 3138. (c) Gable, K. P.; Phan, T. N. *J. Am. Chem. Soc.* **1994**, *116*, 833. (d) Gable, K. P.; Phan, T. N. *J. Am. Chem. Soc.* **1993**, *115*, 3036.

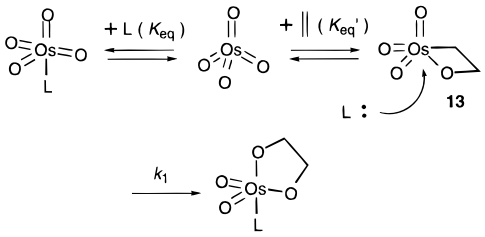

Figure 21. Alternate "[2 + 2]" pathway involving nucleophilic attack of the ligand and synchronous rearrangement.

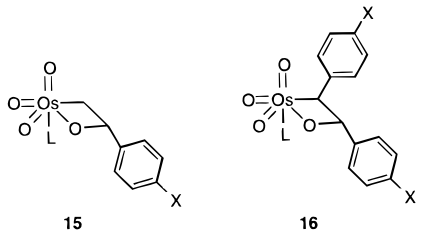

Figure 22. Proposed ligated osmaoxetanes formed from styrene (**15**) or stilbene (**16**).

The net effect of using strongly coordinating tertiary amines to accelerate osmylations should be a marked decrease in the concentration of osmaoxetane **13**, a prediction based on the competition between the alkene and the amine for complexation with the Lewis acidic OsO_4. This competition should slow the rate of osmylation when the reaction is performed in the presence of high concentrations of the amine unless the ligand-promoted rearrangement of osmaoxetane **13** compensates for this effect. With sterically simple amines such as pyridine and quinuclidine where no stabilizing noncovalent interactions between substrate and ligand occur, coordination of the amine could afford synchronous rearrangement to the Os(VI) glycolate (Figure 21). This pathway may also be possible when both alkene and ligand are sterically demanding. The rate expression for this mechanism is kinetically indistinguishable from the rate expression for the "[3 + 2]" pathway.[2b] The reaction rates for this pathway, or any variant of the "[2 + 2]" mechanism, could exhibit inhibition at high amine concentrations, but the extraordinarily rapid and reversible equilibrium for the coordination of the amines to OsO_4 prevents the expected inhibition.[71]

The trajectory for attack of the amine on the osmaoxetane in Figures 19 and 21 is based on computational evidence. It is currently very difficult to model transition states for such complex systems,[72] but calculations using density functional theory (DFT) on ligated ruthenaoxetane intermediates have shown that the complex with the ligand coordinated trans to an oxo group is approximately 3 kcal/mol more stable than the complex with the ligand coordinated trans to the metallaoxetane.[13b] Molecular modeling studies on the ligated metallaoxetane that endeavor to rationalize facial selectivity in the catalytic AD place the alkaloid ligand trans to the oxo group, because it is virtually impossible to rationalize high enantioselectivies with the isomeric complex (i.e., L trans to the metallaoxetane). Osmylations accelerated by achiral and sterically undemanding amines are not bound by the necessity to rationalize enantiofacial selectivity, but coordination of the amine trans to the oxo group should be governed by similar orbital considerations.

The mechanism shown in Figure 21 could produce nonlinear Hammett relationships. The nucleophilic attack of the amine on the osmaoxetane should be susceptible to substrate electronic effects. Electron-donating substituents on the alkene are expected to increase the concentration of the 16-electron osmaoxetane **13**, but they should decrease its electrofugacity and thereby retard amine-accelerated rearrangement. Likewise, electron-withdrawing substituents should decrease the concentration of **13** but make it more electrophilic. The combination of these competing effects may produce a nonlinear Hammett relationship, but it is very unlikely that this could result in faster reaction rates for electron-withdrawing substituents. From the simple perspective of a stepwise mechanism where the component steps can be described by ρ values having different signs (e.g., $\rho_1 < 0$ and $\rho_2 > 0$), the overall reaction rate cannot exhibit a distinct minimum in response to electronic substituents on the alkene.

Therefore, the synchronous ligand addition-rearrangement version of the stepwise mechanism in Figure 21 cannot explain the present Hammett data. Another difficulty in rationalizing the curved Hammett plots by a "[2 + 2]" mechanism arises from the observation of the unusual response to electronic factors with alkenes that should exhibit a strong regiochemical preference in formation of **13** and **14** as well as for alkenes that should show no regiochemical preference. This point is best illustrated by a consideration of the structure of the ligated osmaoxetanes from styrene and stilbene derivatives. The strength and/or migratory aptitude of the carbon−osmium bond in **15** should not be influenced by substituents to the same extent as the analogous bond in **16**. In either case it is not obvious why the presence of the amine ligand (L) should accelerate the rearrangement process for electron-donating *and* electron-withdrawing substituents on the substrate. This argument can be used against the "[2 + 2]" mechanism (Figure 19) via ligated osmaoxetane **14**, but only in reactions accelerated by strongly coordinating amines that afford parabolic Hammett plots. It is necessary to emphasize the different responses to electronic effects between the strongly binding simple amines and the alkaloid ligand. Calculations using ammonia as the ligand indicate that **14** is energetically accessible as a stable intermediate,[13a] but the nonlinear Hammett behavior observed using strongly binding amines is inconsistent with the mechanism in Figure 19. The nearly linear Hammett behavior observed with DHQD-CLB and the different alkenes is consistent with this mechanism. Stabilization of **14** caused by interaction between the aromatic group on the alkenes and the "binding pocket" may explain in part the differences in response to substrate electronic effects between reactions with alkaloid ligands and those using simple tertiary amines with comparable K_{eq} values.

An alternative to the amine-accelerated "[2 + 2]" pathways depicted in Figures 19 and 21 has recently been proposed by Corey.[73] This new mechanism involves rapid and reversible complexation of the alkene to the metal center of the ligand−OsO_4 complex (Figure 23). The premise for this mechanistic proposal arises from the observation of Michaelis−Menten-like kinetic behavior in turnover studies in the heterogeneous, catalytic AD. The recent characterization of the complex between osmium tetroxide and a chelating diamine provides evidence that 20-electron osmium(VIII) complexes such as **17**

(71) The complete expression for the observed rate constant for the mechanism in Figure 21 is: $(k_o + k_1)(k_a)/(k_o + k_{-a} + k_1[L])(1 + K_{eq}[L])$ which simplifies to eq 6 when the assumption that $k_{-a} \gg k_o$ and $k_1[L]$ is made (k_a and k_{-a} are the microscopic rate contants that compose K_{eq}'). Evidence for the rapid and reversible equilibrium K_{eq} was obtaind from low-temperature NMR experiments in which only time-averaged signals were observed using quinuclidine and OsO_4 as low as −100 °C: Sharpless, K. B.; Jacobsen, E. N. Unpublished results.

(72) For recent calculations on the proposed transition states, see: Torrent, M.; Deng, L.; Duran, M.; Sola, M.; Ziegler, T. *Organometallics* **1997**, *16*, 13.

(73) Corey, E. J.; Noe, M. C. *J. Am. Chem. Soc.* **1996**, *118*, 319. Also see ref 86.

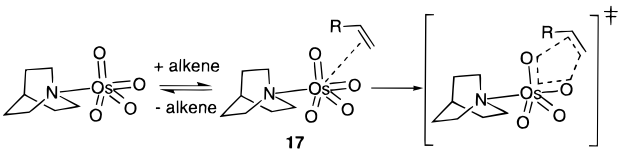

Figure 23. Mechanistic proposals for osmylation via initial complexation of the alkene to the metal center of the OsO_4−amine complex.

may be possible.[74] However, the OsO_4−diamine complex is extremely unstable thermally, and these complexes only achieve stoichiometric enantioselective osmylation of alkenes at very low temperatures. Also, a correlation between the mechanism of these stoichiometric versions using chelating diamines at very low temperatures with the mechanism of the osmylation step in the catalytic AD has not been established.

It is unlikely that the mechanism shown in Figure 23 operates in the catalytic AD at or above 0 °C. The dissociation of ligand from complex **1** is exceptionally rapid,[75] and the formation of **17** would actually consist of two sequential equilibria in which the microscopic rate constants are very great. Rapid dissociation of the amine from complex **1** forms the basis for the "[2 + 2]" pathways (Figures 19 and 21). A direct "[2 + 2]" addition of **1** to the alkene in the rate determining step followed by fast rearrangement to the ligated osmium(VI) glycolate is indistinguishable from the classical "[3 + 2]" pathway. Each of these mechanistic variations fails to provide a satisfactory explanation for the entire range of substrate electronic effects.

A stepwise mechanism involving complexation of an alkene to the Lewis acidic metal center is intuitively more attractive in unaccelerated reactions that have no ligand to coordinate competitively. The Hammett plots for the unaccelerated osmylations reported here are consistent with this interpretation. An evaluation of the response to substrate electronic effects in other alkene oxidations effected by oxygen transfer from transition metal species with one or more oxo groups reveals that many exhibit behavior similar to unaccelerated osmylations. The closely related permanganate oxidations were reported to exhibit almost no response to substituent effects as reported by Wiberg.[76] A study on substituent effects in oxidations of vinylic ethers by permanganate in basic aqueous media reported rate acceleration by both electron-withdrawing and electron-donating groups.[77] Electrophilic oxidations of the same vinylic ethers by OsO_4 in the presence of very low concentrations of pyridine were also reported.[77] Alkyne oxidation by tetrabutylammonium permanganate in methylene chloride has been reported to be accelerated by electron-withdrawing substituents, but it was not clearly demonstrated that the kinetic measurements corresponded to formation of the manganate(V) ester.[78] A recent study reports a direct correlation between the IPs of several different alkenes and the rates of permanganate oxidation.[79] The many different reaction conditions and numerous products formed in permanganate oxidations prevent a simple and direct comparison with osmylation reactions, and the influence of coordinating ligands with permanganate has not been described.

Studies on the kinetics of chromyl chloride oxidations of substituted styrenes revealed a linear Hammett relationship with a ρ value of -1.2,[80] and relative rate studies on structurally different alkenes confirmed this trend.[10a] These reactions have been proposed to proceed by initial formation of a metallaoxetane in direct analogy with formation of the osmaoxetane.[10a] The response to electronic factors in numerous other metal−oxo systems that effect oxidation of alkenes including metallaporphyrins[81] and ruthenium(VI) complexes with tetradentate amine ligands[82] have also been reported. Most of these reactions are proposed to proceed via radical intermediates, as are the catalytic epoxidation reactions using manganese salen complexes.[83] However, an alternate mechanism involving initial, reversible formation of metallaoxetane intermediates has recently been proposed for these oxygen atom transfer processes.[84]

Additional Mechanistic Considerations. Several studies reported here reveal that the extent of the curvature in the Hammett relationships is directly related to the concentration of the amine. The osmylations of substituted styrenes accelerated by 4-picoline in acetonitrile (Figure 8) and the DMAP-accelerated osmylation of *trans*-stilbenes in toluene (Figure 14) and triphenylethylenes in acetonitrile (Supporting Information) clearly illustrate this point. In these cases, the degree of curvature in the Hammett plots decreases as the number of equivalents of accelerating amine decreases. The most dramatic change in curvature occurs in regions corresponding to alkenes bearing electron-withdrawing substituents. This pattern has important implications for the mechanism of the reaction, because it shows that the approach to rate saturation depends on the nature of the alkene in addition to the ligand concentration. The expression that describes the saturation behavior for the "[3 + 2]" pathway (eq 1) predicts Hammett plots of identical shape for any concentration of the accelerating amine so long as the contribution of the unaccelerated reaction to the overall rate remains negligible. The 4-picoline-accelerated osmylations of styrenes (Figure 8) demonstrate most clearly that the unaccelerated osmylations do not contribute to the curvature in the Hammett plots (*vide infra*).

None of the proposed "[2 + 2]" mechanisms provides a general explanation for the parabolic shape of the Hammett plots obtained in the osmylation reactions accelerated by strongly coordinating tertiary amines. Taken together with the concerted "[3 + 2]" mechanism's apparent failure to rationalize the inconsistent changes in the shapes of the curved Hammett plots in response to substrate and solvent effects (Supporting Information) the conclusion must be reached that *none* of the proposed mechanisms is sufficient. In order to accommodate all of the quantifiable data for the stoichiometric osmylations, including the observation of inversion points in modified Eyring plots based on enantioselectivity in stoichiometric AD reactions,[12] it is necessary to consider the possibility that two different mechanisms operate concomitantly.

In this scenario, one of the operative pathways may dominate the reaction under extreme reaction conditions. The accelerated osmylations using strongly binding ligands and alkenes bearing electron-withdrawing substituents exhibit positive ρ values and

(74) Corey, E. J.; Sarshar, S.; Azimioara, M. D.; Newbold, R. C.; Noe, M. C. *J. Am. Chem. Soc.* **1996**, *118*, 7581.

(75) Low temperature ^{13}C NMR studies on the equilibrium for coordination of quinuclidine to OsO_4 have established a minimum rate of $>5 \times 10^3$ s^{-1} for the dissociation of the ligand at −140 °C. Reich, H. J., Sikorsky, W. Personal communication.

(76) Wiberg, K. B.; Geer, R. D. *J. Am. Chem. Soc.* **1966**, *88*, 5827.

(77) Toyoshima, K.; Okuyama, T.; Fueno, T. *J. Org. Chem.* **1980**, *45*, 1600.

(78) Lee. D. G.; Lee, E. L.; Chandler, W. D. *J. Org. Chem.* **1985**, *50*, 4306.

(79) Nelson, D. J.; Henley, R. L. *Tetrahedron Lett.* **1995**, *36*, 6375.

(80) Freeman, F.; Yamachika, N. J. *J. Am. Chem. Soc.* **1970**, *92*, 3730.

(81) Arasasingham, R. D.; He, G.-X.; Bruice, T. C. *J. Am. Chem. Soc.* **1993**, *115*, 7985.

(82) Cheng, W.-C.; Yu, W.-Y.; Li, C.-K.; Che, C.-M. *J. Org. Chem.* **1995**, *60*, 6840.

(83) Jacobsen, E. N. In *Catalytic Asymmetric Synthesis*; Ojima, I., Ed.; VCH Publishers, Inc.: New York, 1993; pp 159−202.

(84) (a) Hamada, T.; Fukuda, T.; Imanishi, H.; Katsuki, T. *Tetrahedron* **1995**, *52*, 575. (b) Bousquet, C.; Gilheany, D. G. *Tetrahedron Lett.* **1995**, *36*, 7739. (c) Norrby, P.-O.; Linde, C.; Åkermark, B. *J. Am. Chem. Soc.* **1995**, *117*, 11035.

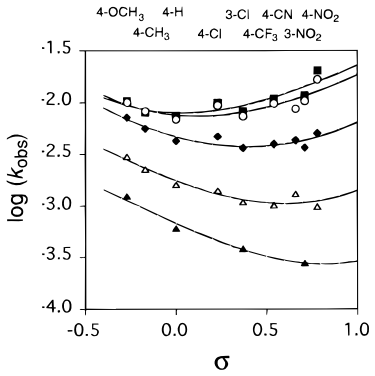

Figure 24. Nonlinear fits of the Hammett plots for the pyridine-accelerated osmylations of styrenes in Table 5 (■ = 4-pyrrolidinopyridine, ○ = DMAP, ◆ = pyridine, △ = 4-cyanopyridine, ▲ = 3,5-dichloropyridine).

therefore suggest a mechanism that proceeds via a "nucleophilic" osmium(VIII) species. The beneficial effect of coordinating tertiary amines in the osmylation of electron-deficient alkenes has been noted previously.[85] A pericyclic mechanism similar to a 1,3-dipolar cycloaddition involving OsO_4−L complex **1** provides the only currently available explanation for the rate increases observed for electron-deficient alkenes. The numerous inconsistencies between experimental data and the behavior predicted by the "[3 + 2]" pathway show that this nucleophilic mechanism cannot be general for all alkene/ligand combinations.

Osmylation reactions performed using lower concentrations of moderate to poorly binding amines are dominated by a mechanism characterized by negative ρ values in response to substrate substituents. This "electrophilic" pathway is at present best rationalized by a stepwise mechanism via an osmaoxetane intermediate. The simultaneous operation of two competing reaction mechanisms can satisfactorily explain the nonlinear Hammett behavior. Figure 24 depicts a nonlinear fit of the Hammett data for the substituted pyridine-accelerated osmylations of styrenes in toluene (Figure 7) based on a mechanistic model where the observed rate constant is the sum of two rate constants for concomitant mechanisms (eq 6). One of the pathways used in the calculated fit obeys a linear Hammett relationship giving a negative ρ value (the electrophilic path),

$$k_{obs} = k_1 + k_2 = k_1^{\circ}10^{\rho_1\sigma} + k_2^{\circ}10^{\rho_2\sigma} \qquad (6)$$

and the other mechanism exhibits linear Hammett behavior giving a positive ρ value (the nucleophilic path). This represents the simplest possible representation of the complex Hammett data described above. The ρ values extracted from the nonlinear fits illustrated in Figure 24 fall in the expected range ($-1 < \rho_1 < 0$, and $0 < \rho_2 < 1$) for osmylation reactions. Of course, the use of eq 6 to fit a curved Hammett plot does not prove the existence of two different mechanisms that follow Hammett relationships with ρ values of opposite signs. A problem that cannot be adequately addressed at this point is whether the "nucleophilic [3 + 2]" pathway will give a linear Hammett plot or a parabolic plot by analogy with 1,3-dipolar cycloaddition reactions. The latter case would mean that the observed nonlinear Hammett plots in osmylations result from the combination of a linear and a parabolic Hammett function. In either case, the simultaneous operation of different mechanisms is consistent with all of the data currently available for stoichiometric osmylations.

(85) Herrmann, W. A.; Eder, S. J.; Scherer, W. *Angew. Chem., Int. Ed. Engl.* **1992**, *31*, 1345.

The implications of these new findings for the controversy surrounding the source of asymmetric induction in the catalytic AD are of special interest. The standard conditions for performing the catalytic AD reaction employ very low concentrations of the alkaloid ligands ([L] = 1×10^{-3} M, where 1 mol % of the ligand and 0.2 mol % of the osmium catalyst are used).[1] The present model studies with DHQD-CLB employ substantially higher concentrations of the alkaloid ligand (5.0×10^{-2}−1.0×10^{-1} M) and a Hammett plot consistent with the electrophilic mechanism was observed. The smaller equilibrium constant for the bisalkaloid ligands in *tert*-butyl alcohol ($K_{eq} = 27\ M^{-1}$ for $(DHQD)_2PHAL$)[2c] and lower concentrations used in the catalytic system provide additional evidence that under normal AD conditions a stepwise mechanism is feasible. The only cases in which a "[2 + 2]" mechanism can be excluded require strongly electron-withdrawing substituents on the alkene in addition to high concentrations of strongly binding amines.

A significant limitation for most studies of the catalytic AD arises because the arguments rely only on the observed enantioselectivities. The debate about the nature of the "binding pocket" is based largely on such inadequate evidence. The current study on electronic effects in stoichiometric osmylations illustrates the remarkable complexity of the Os(VI) glycolate formation step. The catalytic cycle under the heterogeneous AD conditions comprises at least four steps other than glycolate formation: hydrolysis of the Os(VI) glycolate, phase migration, reoxidation to Os(VIII), and another phase migration. Unlike the glycolate-forming step, these additional steps have not been studied in any detail. Hence, mechanistic interpretations based on the rate of alkene consumption in the catalytic AD are suspect because the turnover-limiting step is rarely glycolate formation. For this reason, extreme caution should be exercised when drawing mechanistic conclusions from turnover rates or enantioselectivity in *catalytic* AD reactions.[86]

Conclusion

The present study on electronic effects in stoichiometric osmylations reveals that the amine-accelerated process, belying the apparent simplicity of the overall transformation, is extremely complicated. Studies based on variation of the ligand substituent show that electronic effects can be transmitted directly from the ligand to the metal in the amine−OsO_4 complexes. As expected, the N−Os bond length decreases as the amine becomes more basic. Also, the equilibrium constants for formation of amine−OsO_4 complexes increase when electron-releasing substituents are bound to the amine, and the reduction potentials of solutions containing OsO_4 and amines increase in direct proportion to the coordinating capacity of the ligand. Strangely, these straightforward substituent effects do not manifest themselves in simple linear free energy relationships in reactions with olefins. Hammett plots based on the ceiling rate constants reveal only minor differences in reactivity for pyridines of dramatically different basicity, an outcome that provides inconclusive information about the reaction mechanism.

Investigations of substrate substituent effects through analysis of reaction kinetics reveal unusual Hammett behavior for amine-accelerated osmylations. Parabolic Hammett plots exhibiting distinct minima were obtained for several reaction series employing a variety of tertiary amine ligands and structurally different alkenes. Nonlinearity in the Hammett relationships

(86) The observation of Michaelis−Menten-like kinetic behavior in the catalytic AD reported by Corey and Noe (ref 73) results from a step other than osmylation. Kinetic studies on the stoichiometric AD of styrene under conditions that replicate the organic phase of the catalytic AD reveal that the rate expression is clearly first order in styrene over a wide range of concentrations. Nelson, D. W.; Sharpless, K. B. Unpublished results.

depended on the basicity/equilibrium constant for the amine ligand as well as its concentration. The position of the minima in the Hammet plots shifted toward electron-rich alkenes as the equilibrium constant increased, but exceptions to this trend were noted when the structure of the amine changed. These nonlinear Hammett relationships stand in marked contrast to the linear free energy relationships observed in unaccelerated osmylations. Attempts were made to rationalize this behavior by comparison between the proposed concerted "[3 + 2]" mechanism and analogous 1,3-dipolar cycloadditions in organic systems. Severe inconsistencies between the experimental data and theory were noted, but the "[3 + 2]" pathway offers one possible explanation for the segment of the Hammett plot characterized by a positive ρ value (the nucleophilic region).

Attempts to rationalize the curved Hammett plots using variations of the stepwise "[2 + 2]" pathway failed because a change in the rate determining step for a sequential pathway cannot afford a Hammett relationship with a distinct minimum. The dependence of the extent of curvature in the Hammett plots on the concentration of the amine ligands strongly implicates the operation of two different ligand-accelerated pathways. The nucleophilic pathway requires both strongly coordinating amines *and* electron-withdrawing substituents on the substrate. The electrophilic pathway dominates reactivity under conditions employing lower concentrations of moderately binding amines as well as for most alkyl substituted alkenes. A Hammett plot dominated by a process with a negative ρ value was determined for stoichiometric osmylations using alkaloid ligands, and this electrophilic pathway is consistent with a stepwise "[2 + 2]" mechanism. In summary, the results to date indicate that the selectivity-determining step of the catalytic AD, which employs low concentrations of moderately binding bisalkaloid ligands, proceeds by the electrophilic pathway which at present is most consistent with the ligated osmaoxetane intermediate previously proposed.[87]

Experimental Section

NMR spectra were recorded on a Bruker AC-250 spectrophotometer. Infrared spectra were recorded on a Nicolet 510 FT-IR spectrophotometer. UV−visible spectra were obtained on a Cary 4 spectrophotometer with a thermostatted cell block. The substituted pyridines and DHQD-CLB were obtained from commercial sources as were the substituted styrenes. All compounds were purified by standard methods and analyzed by ^{1}H NMR spectroscopy before use.

General Procedure for the Determination of Equilibrium Constants for the Coordination of Substituted Pyridines to OsO_4. A modified titration procedure was followed. The UV−visible spectrum of a solution containing OsO_4 ($1.00-3.15 \times 10^{-3}$ M) was obtained using a reference consisting of only solvent. A series of solutions containing OsO_4 ($1.00-3.15 \times 10^{-3}$ M) and the substituted pyridine (2−400 equiv) were prepared, and the UV−visible spectra of these solutions were obtained using reference solutions containing the amine (no OsO_4). Lower concentrations of OsO_4 and the pyridines were used for the pyridine derivatives with large binding constants and vice versa. Spectra were obtained for at least five different solutions, and the equilbrium constants were calculated by a single-reciprocal graphic technique (from a linear least-squares fit of a plot of [L]/ΔA vs [L]) or a double-reciprocal graphic technique (from a linear least squares fit of a plot of 1/ΔA vs 1/ΔL).

General Procedure for the Determination of Equilibrium Constants for Coordination of Substituted Quinuclidines to OsO_4. A 500 mL aliquot of a solution the ligand in toluene-d_8 was transferred to a 5 mm NMR tube, and the ^{13}C NMR spectrum was recorded. An aliquot (10−20 mL) of a solution containing a different ligand (∼0.2 equiv) in toluene-d_8 was added, and the ^{13}C NMR spectrum was recorded. Additional aliquots of the solution containing the different ligand were added until no change in the spectrum was detected. Relative binding constants were obtained by plotting $(\delta L_2 - \delta L_{2c})/(\delta L_{2o} - \delta L_2)$ vs $(\delta L_1 - dL_{1c})/(\delta L_{1o} - \delta L_1)$ where δL_1 and δL_2 are the observed chemical shifts for ligands L_1 and L_2, δL_{1o} and δL_{2o} are the chemical shifts of noncomplexed ligands L_1 and L_2, and δL_{1c} and δL_{2c} are the chemical shifts of the fully complexed ($L-OsO_4$) ligands as determined separately in the presence of a large excess of OsO_4. The K_{rel} value for the two ligands was obtained from the reciprocal of the slope.

General Procedure for Kinetic Analysis of Osmylation Reactions by UV−Visible Spectroscopy. To a 3-mL quartz cuvette with a Teflon stopper were added via syringe stock solutions of the alkene and the amine ligand in anhydrous solvent. Additional solvent was added via syringe to dilute to a volume of 2 mL (minus the volume of the OsO_4 stock solution added later). The cuvette was placed in the thermostatted cell block of the spectrophotometer for several minutes to reach thermal equilibrium. A small volume (typically 10−25 mL) of a stock solution of OsO_4 in the solvent was added quickly, the solution was shaken vigorously, and measurements were started. Initially, wavelength scans were made at regular intervals to determine the wavelengths at which to monitor the reactions. Isosbestic points were observed in most reactions. Each reaction was monitored for a period of time corresponding to 4−8 half-lives. The observed pseudo-first-order rate constants were calculated using the Varian (Cary 04E) software program.

General Procedure for the Preparation of Bispyridine Osmium(VI) Glycolates. To a 15-mL, round-bottomed flask containing a magnetic stir bar were added via syringe ∼4 mL of a solution of the appropriate amine (∼0.5 M) in toluene and ∼1 mL of a solution of OsO_4 (∼0.2 M) in toluene. The styrene (∼0.22 mmol) was added neat via syringe, and the golden/orange solution turned red/brown immediately. The reaction solution was stirred at room temperature under an atmosphere of dry N_2 until a red/brown precipitate formed. If no precipitate formed after 2 h, then pentane was added dropwise until the reaction mixture became heterogeneous. The precipitate was collected by vacuum filtration on a fine frit, and the product was washed with several portions of pentane. The solid usually contained a substantial amount of toluene, so anhydrous dichloromethane was added to dissolve the solid, and the solvents were removed under high vacuum to give powdery, brown solids.

[(4′-Methoxyphenyl)ethane-1,2-diolato]dioxodi(4-*N*-pyrrolidinopyridine)osmium(VI): ^{1}H NMR ($CDCl_3$) δ 8.37 (dd, J = 6.9, 6.9 Hz, 4H), 7.49 (d, J = 8.6 Hz, 2H), 6.86 (d, J = 8.6 Hz, 2H), 6.38 (dd, J = 7.7, 7.7 Hz, 4H), 5.51 (dd J = 9.9, 4.4 Hz, 1H), 4.55 (dd, J = 10.0, 4.5 Hz, 1H), 4.40 (dd, J = 10.0, 10.0 Hz, 1H), 3.78 (s, 3H), 3.42−3.35 (m, 8H), 2.07−2.00 (m, 8H).

Dioxo(phenylethane-1,2-diolato)di(4-*N*-pyrrolidinopyridine)osmium(VI): ^{1}H NMR ($CDCl_3$) δ 8.37 (dd, J = 5.8, 5.8 Hz, 4H), 7.57 (d, J = 7.4 Hz, 2H), 7.32 (dd, J = 7.5, 7.3 Hz, 2H), 7.20 (dd, J = 6.8, 6.8 Hz, 1H), 6.38 (dd, J = 6.8, 6.8 Hz, 4H), 5.55 (dd, J = 10.0, 4.4 Hz, 1H), 4.59 (dd, J = 10.0, 4.4 Hz, 1H), 4.40 (dd, J = 10.0, 10.0 Hz, 1H), 3.42−3.35 (m, 8H), 2.06−2.00 (m, 8H).

[(3′-Chlorophenyl)ethane-1,2-diolato]dioxodi(4-*N*-pyrrolidinopyridine)osmium(VI): ^{1}H NMR ($CDCl_3$) δ 8.38−8.34 (m, 4H), 7.59 (br s, 1H), 7.41 (d, J = 7.2 Hz, 1H), 7.25−7.17 (m, 2H), 6.41−6.37 (m, 4H), 5.50 (dd, J = 9.8, 4.3 Hz, 1H), 4.59 (dd, J = 10.1, 4.5 Hz, 1H), 4.35 (dd, J = 10.0, 10.0 Hz, 1H), 3.43−3.37 (m, 8H), 2.06−2.02 (m, 8H).

[(4′-Nitrophenyl)ethane-1,2-diolato]dioxodi(4-*N*-pyrrolidinopyridine)osmium(VI): ^{1}H NMR ($CDCl_3$) δ 8.35 (d, J = 5.6 Hz, 4H), 8.17 (d, J = 8.6 Hz, 2H), 7.73 (d, J = 8.6 H, 2H), 6.39 (d, J = 7.0 Hz, 4H), 5.57 (dd, J = 9.2, 4.6 Hz, 1H), 4.65 (dd, J = 10.1, 4.6 Hz, 1H), 4.34 (dd, J = 9.7, 9.7 Hz, 1H), 3.42−3.39 (m, 8H), 2.06−2.02 (m, 8H).

Di[4-(*N*,*N*-dimethylamino)pyridine][(4′-Methoxyphenyl)ethane-1,2-diolato]dioxoosmium(VI): ^{1}H NMR ($CDCl_3$) δ 8.40 (dd, J = 6.9, 6.9 Hz, 4H), 7.48 (d, J = 8.5 Hz, 2H), 6.86 (d, J = 8.6 Hz, 2H), 6.50 (dd, J = 7.8, 7.8 Hz, 4H), 5.51 (dd, J = 10.1, 10.1 Hz, 1 H), 4.55 (dd, J = 10.1, 4.5 Hz, 1H), 4.40 (dd, J = 10.1, 10.1 Hz, 1H), 3.78 (s, 3H), 3.09 (s, 6H), 3.07 (s, 6H).

(87) See ref 10b and references cited therein for the latest refinements in this model.

Di[4-(*N*,*N*-dimethylamino)pyridine][(3′-Nitrophenyl)ethane-1,2-diolato]dioxoosmium(VI): ^{1}H NMR ($CDCl_3$) δ 8.44 (s, 1H), 8.39 (dd, J = 7.4, 2.4 Hz, 4H), 8.07 (dd, J = 8.1, 1.3 Hz, 1H), 7.89 (d, J = 7.6 Hz, 1H), 7.46 (dd, J = 7.9, 7.9 Hz, 1H), 6.52 (d, J = 7.2 Hz, 4H), 5.57 (dd, J = 9.3, 4.5 Hz, 1H), 4.66 (dd, J = 10.1, 4.5 Hz, 1H), 4.37 (dd, J = 9.8, 9.7 Hz, 1H), 3.10 (s, 12H).

[(4′-Methoxyphenyl)ethane-1,2-diolato]dioxodipyridineosmium-(VI): ^{1}H NMR ($CDCl_3$) δ 8.94 (br s, 4H), 7.88−7.85 (m, 2H), 7.51−7.46 (m, 4H), 7.47 (d, J = 8.5 Hz, 2H), 6.88 (d, J = 8.6 Hz, 2H), 5.55 (dd, J = 9.8, 4.7 Hz, 1H), 4.57 (dd, J = 10.2, 4.8 Hz, 1H), 4.47 (dd, J = 10.0, 10.0 Hz, 1H), 3.78 (s, 3H).

Dioxo(phenylethane-1,2-diolato)dipyridineosmium(VI): ^{1}H NMR ($CDCl_3$) δ 8.96−8.94 (m, 4H), 7.90−7.85 (m, 2H), 7.56−7.49 (m, 6H), 7.34 (dd, J = 7.4, 7.2 Hz, 2H), 7.27−7.21 (m, 1H), 5.59 (dd, J = 10.0, 4.6 Hz, 2H), 4.61 (dd, J = 10.2, 4.7 Hz, 1H), 4.48 (dd, J = 10.1, 10.1 Hz, 1H).

[(3′-Chlorophenyl)ethane-1,2-diolato]dioxodipyridineosmium-(VI): ^{1}H NMR ($CDCl_3$) δ 8.94 (d, J = 5.2 Hz, 4H), 7.91−7.87 (m, 2H), 7.56−7.49 (m, 5H), 7.40 (d, J = 7.0 Hz, 1H), 7.29−7.22 (m, 2H), 5.54 (dd, J = 9.9, 4.6 Hz, 1H), 4.60 (dd, J = 10.2, 4.6 Hz, 1H), 4.42 (dd, J = 10.1, 10.0 Hz, 1H).

[(4′-Nitrophenyl)ethane-1,2-diolato]dioxodipyridineosmium-(VI): ^{1}H NMR ($CDCl_3$) δ 8.94 (d, J = 3.5 Hz, 4H), 8.20 (d, J = 8.7 Hz, 2H), 7.91 (dd, J = 7.1, 7.1 Hz, 2H), 7.71 (d, J = 8.7 Hz, 2H), 7.54 (dd, J = 6.9, 6.9 Hz, 4H), 5.62 (dd, J = 9.4, 4.6 Hz, 1H), 4.67 (dd, J = 10.1, 4.7 Hz, 1H), 4.41 (dd, J = 9.8, 9.8 Hz, 1H).

Di(4-cyanopyridine)[(4′-methoxyphenyl)ethane-1,2-diolato]dioxoosmium(VI): ^{1}H NMR ($CDCl_3$) δ 9.02 (d, J = 5.5 Hz, 4H), 7.76 (d, J = 5.4 Hz, 4H), 7.41 (d, J = 8.6 Hz, 2H), 6.88 (d, J = 8.7 Hz, 2H), 5.53 (dd, J = 9.6, 5.0 Hz, 1H), 4.54 (dd, J = 9.6, 5.0 Hz, 1H), 4.47 (dd, J = 9.6, 5.0 Hz, 1H), 3.79 (s, 3H).

Di(4-cyanopyridine)[(4′-methylphenyl)ethane-1,2-diolato]dioxoosmium(VI): ^{1}H NMR ($CDCl_3$) δ 9.13 (d, J = 6.5 Hz, 4H), 7.76 (d, J = 6.6 Hz, 4H), 7.37 (d, J = 8.0 Hz, 2H), 7.16 (d, J = 7.9 Hz, 2H), 5.44 (dd, J = 9.7, 4.9 Hz, 1H), 4.57 (dd, J = 10.3, 4.9 Hz, 1H), 4.48 (dd, J = 10.1, 10.1 Hz, 1H), 2.34 (s, 3H).

General Procedure for the Preparation of Bis(quinuclidine)-osmium(VI) Glycolates. To a 15-mL, round-bottomed flask containing a magnetic stir bar were added via syringe ∼4 mL of a solution of the appropriate amine (∼0.5 M) in toluene and ∼1 mL of a solution of OsO_4 (∼0.2 M) in toluene. The styrene (∼0.22 mmol) was added neat via syringe, and the orange-red solution turned dark green immediately. The reaction solution was stirred at room temperature under an atmosphere of dry N_2 for 4−6 h. The solvent, excess styrene, and quinuclidine were removed under high vacuum to give a metallic green solid. The residual toluene was removed by dissolving the solid in a small amount of $CDCl_3$ and then removing the solvent under vacuum.

Bis(quinuclidine)[(4′-methylphenyl)ethane-1,2-diolato]dioxoosmium(VI): ^{1}H NMR ($CDCl_3$) δ 7.24 (d, J = 7.9 Hz, 2H), 7.16 (d, J = 8.1 Hz, 2 H), 5.07 (dd, J = 9.7, 4.8 Hz, 1H), 4.12 (dd, J = 10.4, 4.9 Hz, 1H), 3.98 (dd J = 10.1, 10.0 Hz, 1H), 3.16−3.10 (m, 12H), 2.36 (s, 3H), 1.98−1.93 (m, 12H), 1.73−1.66 (m, 12H).

Bis(quinuclidine)[(4′-[trifluoromethyl]phenyl)ethane-1,2-diolato]-dioxoosmium(VI): ^{1}H NMR ($CDCl_3$) δ 7.59 (d, J = 8.2 Hz, 2H), 7.48 (d, J = 8.1 Hz, 2 H), 5.18 (dd, J = 9.5, 4.8 Hz, 1H), 4.12 (dd, J = 10.2, 4.9 Hz, 1H), 3.95 (dd J = 9.9, 9.9 Hz, 1H), 3.18−3.11 (m, 12H), 1.99−1.94 (m, 12H), 1.74−1.67 (m, 12H).

Bis(quinuclidine)[(4′-nitrophenyl)ethane-1,2-diolato]dioxoosmium(VI): ^{1}H NMR ($CDCl_3$) δ 8.18 (d, J = 8.7 Hz, 2H), 7.57 (d, J = 8.8 Hz, 2 H), 5.32 (dd, J = 9.5, 4.7 Hz, 1H), 4.22 (dd, J = 10.0, 4.7 Hz, 1H), 4.02 (dd J = 9.8, 9.8 Hz, 1H), 3.10−3.04 (m, 12H), 1.90−1.85 (m, 12H), 1.67−1.60 (m, 12H).

General Procedure for the Stoichiometric Asymmetric Dihydroxylation of Styrenes. To a 25-mL, round-bottomed flask were added via syringe stock solutions of DHQD-CLB (∼0.1 M in toluene) and OsO_4 (∼0.35 M in toluene). The resulting yellow-orange solution contained 0.500 mmol of OsO_4 and 1.00 mmol of DHQD-CLB in 11.2 mL of toluene. The styrene (2.50 mmol) was added neat via syringe, the flask was stirred for 1−2 min, and the homogeneous solution was allowed to stand at room temperature. A dark green color appeared as the osmium(VI) glycolate formed. The reactions were allowed to stand for 1−24 h (longer reaction times were allowed for styrenes bearing electron-withdrawing substituents). The diols were liberated from the osmium complexes by bubbling $H_2S_{(g)}$ through the reaction solution for a period of 5−10 min at 0 °C. The black osmium residue was removed by filtration through a plug of Celite, and the diols were purified by flash chromatography (silica gel/2:1 ethyl acetate:hexanes). Each diol was isolated in >90% yield. The standard conditions recommended for the AD of terminal alkenes were used to prepare the styrene diols: styrene (1.00 mmol), $K_2OsO_2(OH)_4$ (0.2 mol %), DHQD-CLB (1.0 mol %), $K_3Fe(CN)_6$ (3.00 mmol), and K_2CO_3 (3.00 mmol) in 1:1 *tert*-butyl alcohol:water at 25 °C.

The enantiomeric excesses (% ee's) of the resultant diols were determined by chiral HPLC using the following conditions (column; solvent; flow): *p*-methoxystyrene diol (Chiralcel OB-H; 3% isopropyl alcohol, 97% hexane; 1.0 mL/min); *p*-methylstyrene diol (Chiralcel OB-H; 2% isopropyl alcohol, 98% hexane; 1.0 mL/min); styrene diol (Chiralcel OB-H; 10% isopropyl alcohol, 90% hexane; 0.5 mL/min); *p*-chlorostyrene diol, bis benzoate (Chiralpak AD; 10% isopropyl alcohol, 90% hexane; 0.8 mL/min); *m*-chlorostyrene diol (Chiralcel OB-H; 1% isopropyl alcohol, 99% hexane; 0.9 mL/min); *p*-(trifluoromethyl)styrene diol, bis benzoate (Chiralpak AD; 10% isopropyl alcohol, 90% hexane; 0.8 mL/min); *m*-nitrostyrene diol (Chiralpak AD; 2% isopropyl alcohol, 98% hexane; 1.0 mL/min); *p*-nitrostyrene diol (Chiralpak AD; 2% isopropyl alcohol, 98% hexane; 1.0 mL/min).

Acknowledgment. Dedicated to Nelson Leonard, inspiring organic chemist and unparalleled man of science, on the occasion of his 80th birthday. Helpful discusions with Professors Charles Perrin (University of California, San Diego), Dennis H. Evans (University of Delaware), M. G. Finn (University of Virginia), and Mr. Atsushi Makita are gratefully acknowledged. We thank Professor Michael Sailor (University of California, San Diego) for the use of his electrochemical apparatus as well as for help in interpreting the results. Dr. Raj K. Chadha (The Scripps Research Institute) performed the crystal structure determinations. A.E.R. thanks NSERC (Canada) for a 1967 Science and Engineering Scholarship. H.C.K. thanks D.F.G. for a postdoctoral fellowship. A.G. thanks Studien-stiftung des Deutschen Volkes for a BASF fellowship. Financial support was provided by the National Science Foundation (CHE-8903218, CHE-9296055, and CHE-9531152), the National Institutes of Health (GM28384), the W. M. Keck Foundation, and the Skaggs Institute for Chemical Biology.

Supporting Information Available: Derivations of rate expressions; representative UV−visible and NMR spectroscopic data; electrochemical data; experimental and structural information for the X-ray crystal structures of **2**, **3**, and **4**; "ceiling" rate constant calculations; tables of kinetic data for all reported Hammett studies; and description of nonlinear fitting procedure (56 pages). See any current masthead page for ordering and Internet access instructions.

JA961464T